Dual Pol Snow QPE

Petar Bukovčić, Jian Zhang, and
Wolfgang Hanft

TAC meeting,
25 March 2022, Norman OK

Summary of Z(S) relations for dry snow listed in the literature and utilized by the WSR-88D network in the USA

Source	Z(S) relation for dry snow
Gunn and Marshall (1958)	Z = 448 S^2
Sekhon and Srivastava (1970)	Z = 399 S^2.21
Ohtake and Hemni (1970)	Z = (90 – 739) S^(1.5 – 1.7)
Puhakka (1975)	Z = 235 S^2
Koistinen et al. (2003)	Z = 400 S^2
Matrosov et al. (2009)	Z = (100 – 130) S^(1.3 – 1.55)
Huang et al. (2010)	Z = (106 – 305) S(^1.11 – 1.92)
Saltikoff et al. (2010)	Z = 100 S^2
Szyrmer and Zawadzki (2010)	Z = 494 S^1.44
Wolfe and Snider (2012)	Z = 110 S^2
Huang et al. (2015)	Z = (130 – 209) S^(1.44 – 1.81)
Von Lerber et al. (2017)	Z = (53 – 782) S^(1.19 - 1.61)
WSR-88D, Northeast	Z = 120 S^2
WSR-88D, Great Lakes	Z = 180 S^2
WSR-88D, North Plains / Upper Midwest	Z = 180 S^2
WSR-88D, High Plains	Z = 130 S^2
WSR-88D, Inter-mountain West	Z = 40 S^2
WSR-88D, Sierra Nevada	Z = 222 S^2

- The variability of the multiplier in the power-law relations is an order of magnitude!
- Very little progress has been made in radar measurements of snow during last decades

Basic formulas

Ice water content

$$IWC = \frac{\pi}{6}\int \rho_s(D) D^3 N(D) dD \sim M_2$$

Snow rate

$$S = 6\,10^{-4}\pi \int_0^{D_{\max}} \frac{\rho_s(D)}{\rho_w} D^3 V_t^{(s)}(D) N(D) dD \sim M_{2+\gamma}$$

Radar reflectivity

$$Z = \frac{|K_i|^2}{|K_w|^2} \int_0^{D_{\max}} \frac{\rho_s^2(D)}{\rho_i^2} D^6 N(D) dD \sim M_4$$

$$M_n = \int D^n N(D) dD$$

$$S \sim f_{rim}^{0.12} N_{0s}^{0.35} Z^{0.62}$$

The multiplier in the S(Z) relation changes more than an order of magnitude because N0s varies 4 orders of magnitude

Snow size distribution

$$N(D) = N_{0s} \exp(-\Lambda_s D)$$

Snow density

$$\rho_s(D) = \alpha_u f_{\text{rim}} D^{-1}$$

frim is the degree of riming

Snow fall velocity

$$V_t^{(s)} \sim D^{\gamma}$$

Analysis of snow disdrometer data

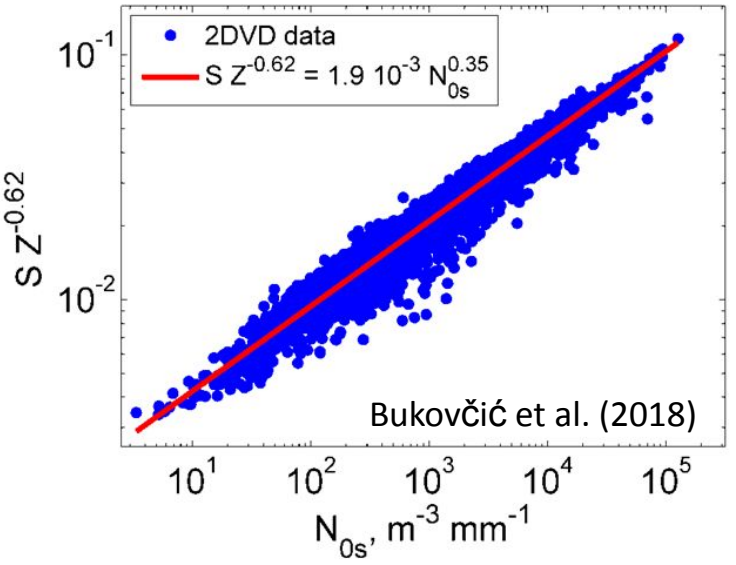

Polarimetric algorithms for snow estimation

Specific differential phase

$$K_{\mathrm{DP}} = \frac{0.27\pi}{\lambda \rho_i^2}\left(\frac{\varepsilon_{\mathrm{i}} - 1}{\varepsilon_{\mathrm{i}} + 2}\right)^2 F_{shape} F_{orinet} \int \rho_s^2(D) D^3 N(D) dD \sim M_1$$

Z is proportional to the 4th moment of snow SD whereas KDP is proportional to its 1st moment

$$S(K_{DP}, Z) = \frac{27.9\times10^{-3}}{(F_s F_o)^{0.615}}\left(p_0 / p\right)^{0.5} (K_{DP}\lambda)^{0.615} Z^{0.33}$$

$$IWC(K_{DP}, Z) = \frac{10.2\times10^{-3}}{\left(F_s F_o\right)^{0.66}}(K_{DP}\lambda)^{0.66} Z^{0.28}$$

Bukovčić et al. (2020)

$$S(IWC) = 2.73\left(p_0 / p\right)^{0.5} IWC\, D_m^{\gamma} \qquad V_t^{(s)} \sim D^{\gamma}$$

$$D_m(K_{DP}, Z) = 1.24\left(\frac{Z F_o F_s}{K_{DP}\lambda}\right)^{1/3}$$

Ryzhkov et al. (2018)

- All polarimetric relations are less sensitive to the SD variability than IWC(Z) or S(Z) relations
- The S(KDP,Z) and IWC(KDP, Z) estimates are prone to the variability of particle shape and orientation

Shape factor

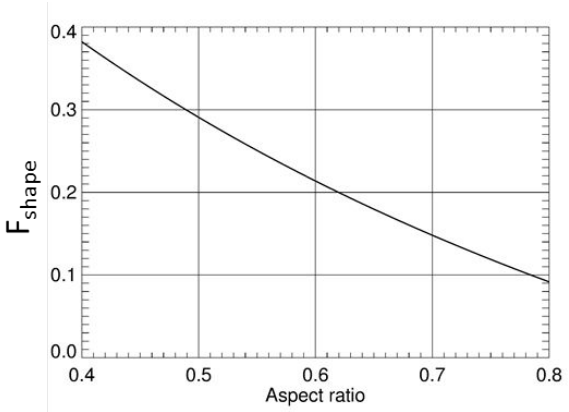

Orientation factor

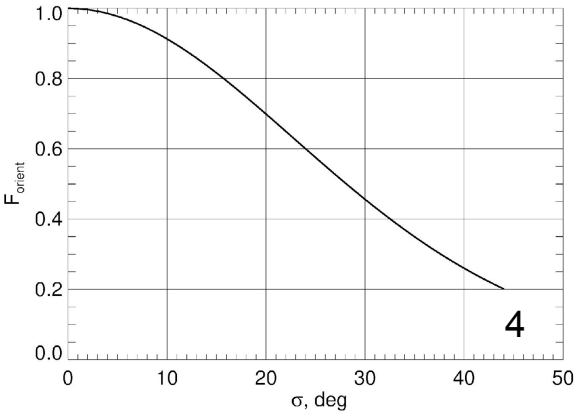

Radar snow relations used in this study

$$S(Z) = 0.091\, Z^{0.5}$$ Eastern US

$$S(K_{DP}, Z) = \frac{27.9\times10^{-3}}{(F_s F_o)^{0.615}} \left(p_0 / p\right)^{0.5} (K_{DP}\lambda)^{0.615} Z^{0.33}$$ Bukovčić et al. (2020)

$$S(IWC) = 2.73\left(p_0 / p\right)^{0.5} IWC(K_{DP}, Z)\, D_m(K_{DP}, Z)^{\gamma}$$ - ongoing research

- ***KDP is low and noisy in snow at S band, therefore, additional spatial averaging is required to obtain robust estimates of KDP (and other pol. variables)***
- ***Recently introduced radar products – Quasi-Vertical Profiles (QVPs), range-defined QVP (RD-QVPs), and Column Vertical Profiles (CVPs) imply aggressive spatial averaging and represent radar data in a height vs time format***

QVP

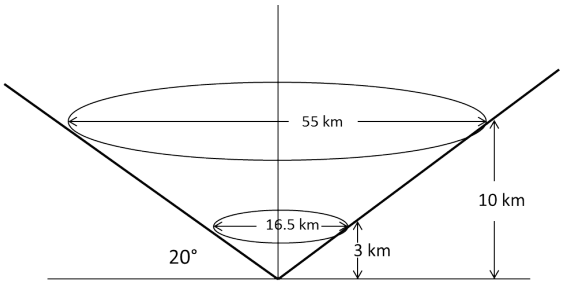

Ryzhkov et al. (2016)

RD-QVP

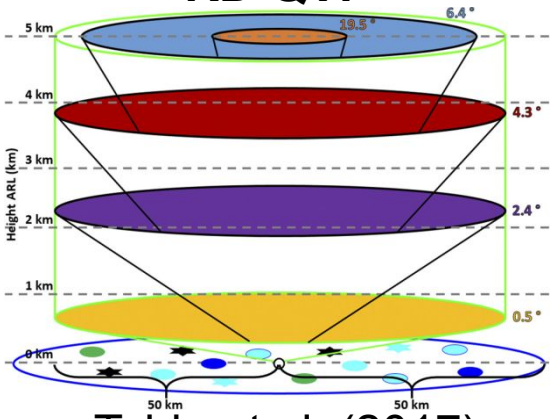

Tobin et al. (2017)

CVP

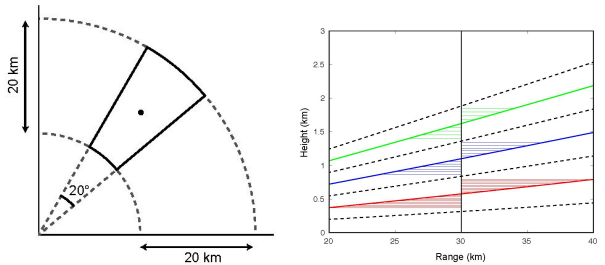

Murphy et al. (2020)

Snowstorm Gail, 2020-12-17

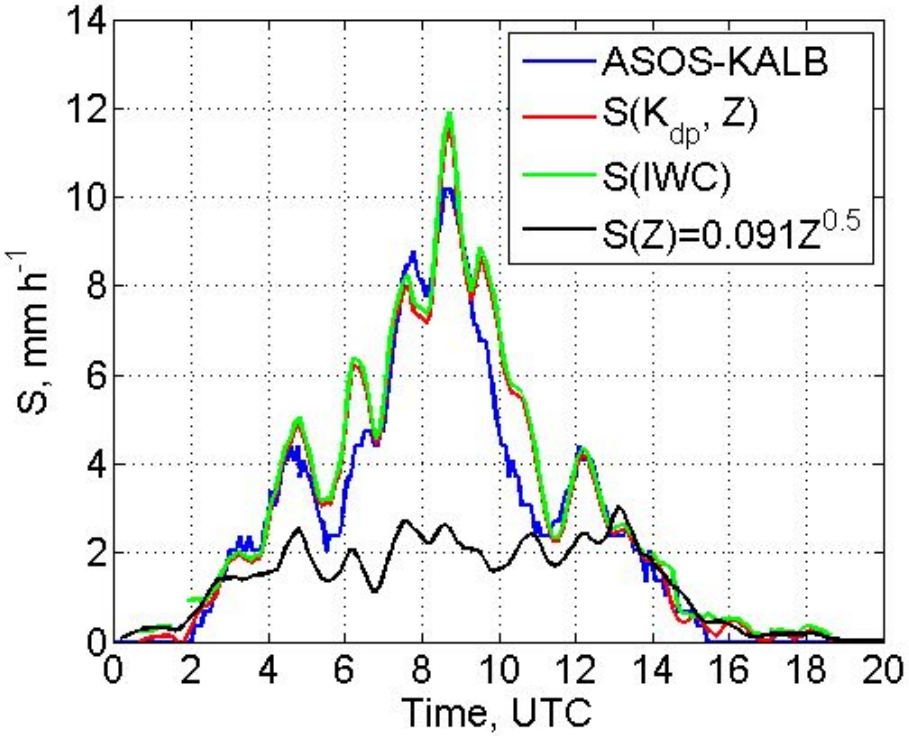

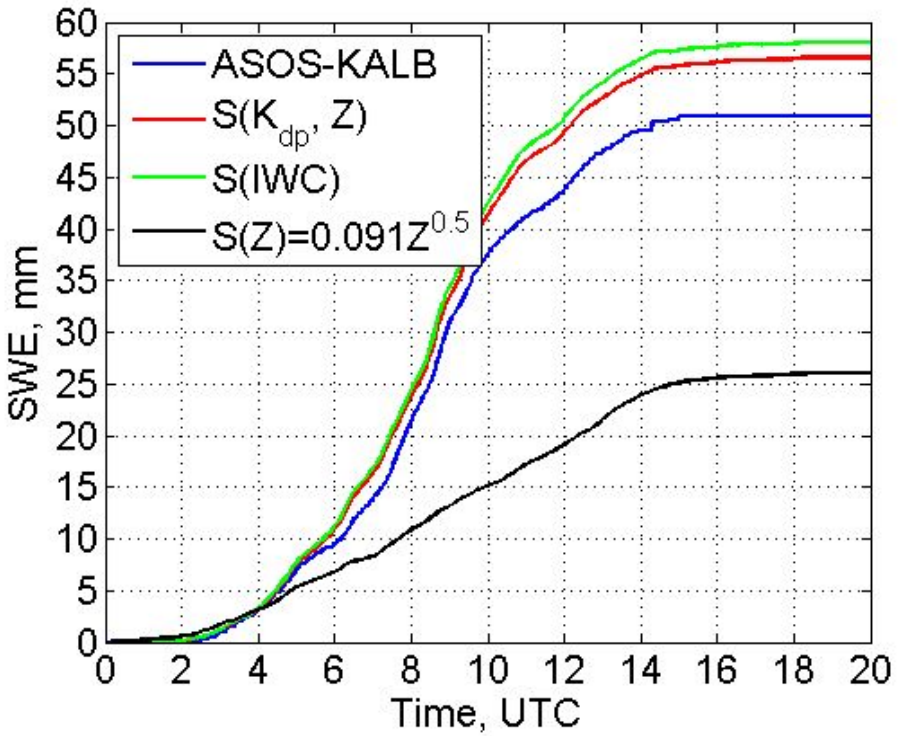

Snowfall rate (mm h^{-1}) / acc. (mm), KENX CVP (250 m AGL) – ASOS KALB (~ 29 km distance from KENX)

Oklahoma ice storm, 2020-10-26 (estimation of snow in stratiform rain)

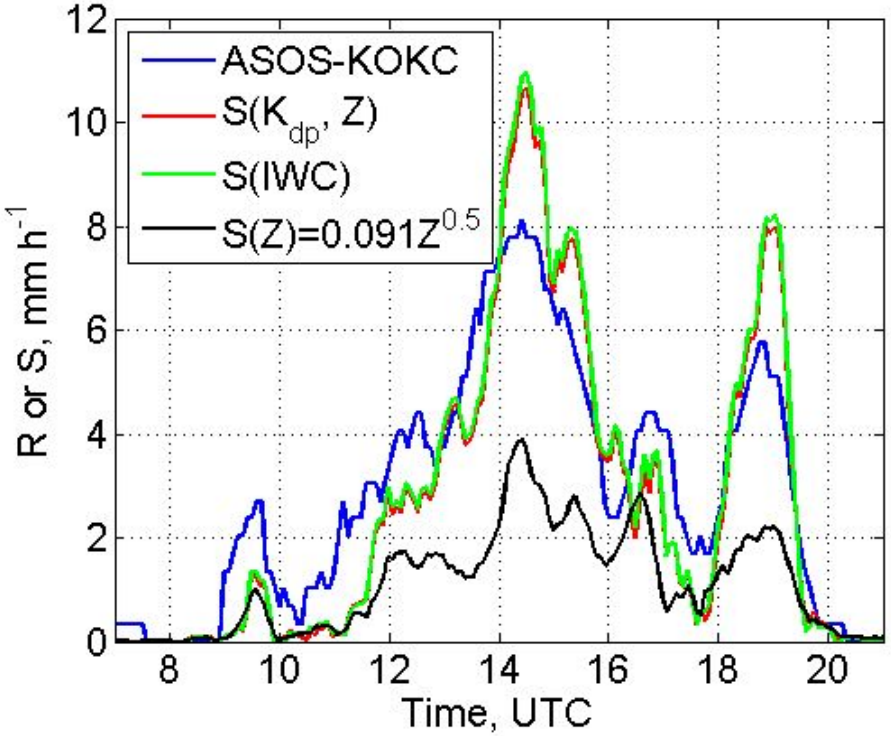

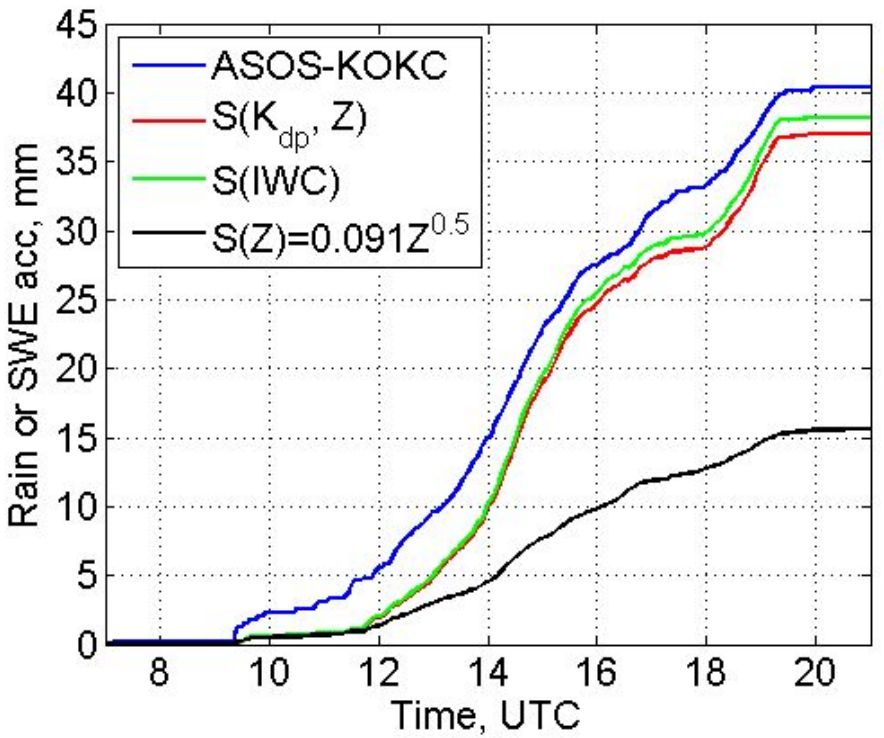

Snowfall or Rainfall rate (mm h^{-1}) / acc. (mm), KTLX CVP (~3500 m AGL) – ASOS KOKC (~ 30 km distance from KTLX)

ICICLE (aircraft obs.), 2019-02-23

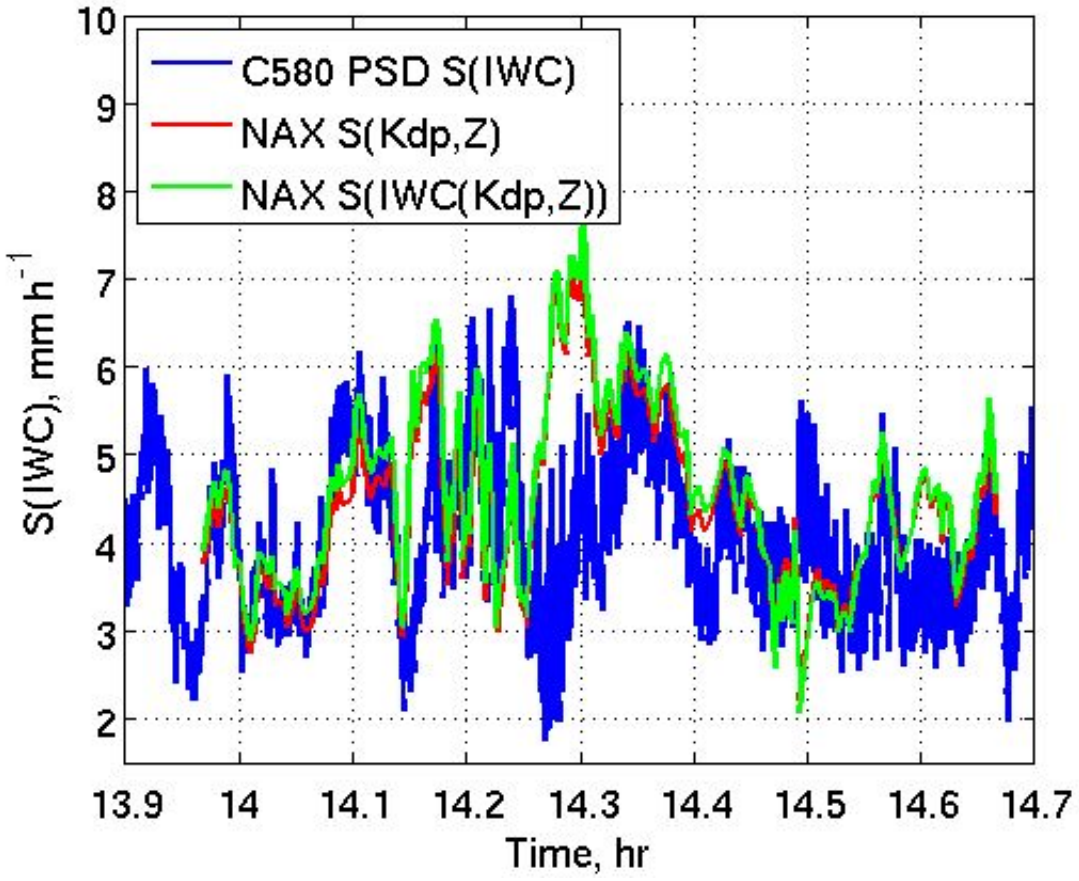

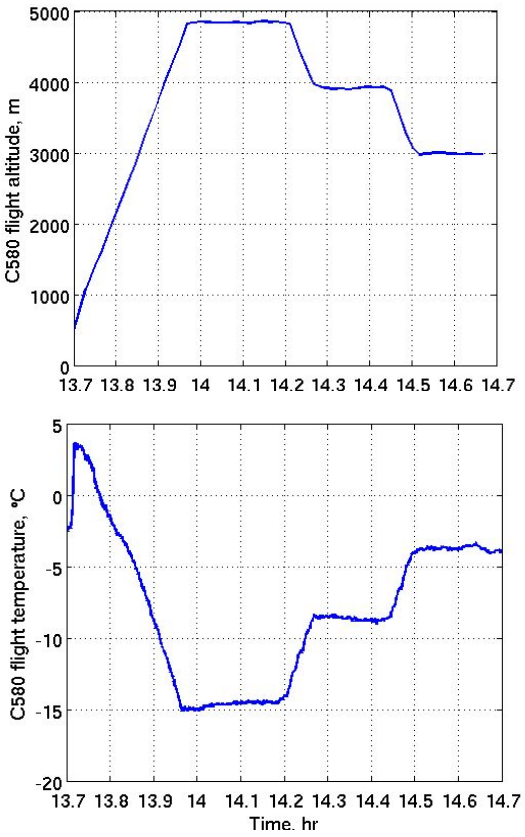

Alt. (m)

T (˚C)

Snowfall rate (mm h^{-1}), C580 PSD (2DC, HVPS probes) – NAX (pol. X-band radar)

Case study analysis

- 30 events selected for analysis
- Events from all across the CONUS
- Varying snowfall totals from a few inches to 12”+
- 24-hour QPE compared to 24-hour CoCoRaHS gauge reports
- Evaluation metrics:
  - Mean Bias Ratio: $MBR = \bar{Q}/\bar{G}$; where:
    - $\bar{Q} = \frac{\sum_{i=1}^{N} Q_i}{N}$, $\bar{G} = \frac{\sum_{i=1}^{N} G_i}{N}$
    - Q_i and G_i are the i^{th} 24-hour QPE and gauge observations
  - Correlation Coefficient: $CC = \frac{\sum_{i=1}^{N}(Q_i-\bar{Q})(G_i-\bar{G})}{\sqrt{\sum_{i=1}^{N}(Q_i-\bar{Q})^2 \sum_{i=1}^{N}(G_i-\bar{G})^2}}$;
  - Mean Absolut Error: $MAE = \frac{1}{N}\sum_{i=1}^{N}|Q_i - G_i|$

Date	Radar	Date	Radar
20170315	KCXX	20191112	KDTX
20170315	KGYX	20191126	KFTG
20180303	KENX	20191202	KENX
20180314	KBOX	20191216	KTWX
20180314	KGYX	20191216	KEAX
20190223	KFTG	20191216	KLSX
20190223	KPUX	20191216	KILX
20191011	KMBX	20191231	KMPX
20191011	KBIS	20191231	KARX
20191012	KMVX	20200209	KFSD
20191012	KMBX	20200209	KMPX
20191012	KBIS	20200209	KARX
20191028	KFTG	20200210	KARX
20191028	KPUX	20200210	KGRB
20191028	KCYS	20200210	KMKX

Equations tested

- Bukovčić et al. 2018:

$$S(K_{DP}, Z) = 1.48 K_{DP}^{0.615} Z^{0.33}$$

- Bukovčić et al. 2020:

$$S(K_{DP}, Z) = \frac{27.9 \times 10^{-3}}{(F_o F_s)^{0.615}} \left(\frac{p_0}{p} \right)^{0.5} (K_{DP} \lambda)^{0.615} Z^{0.33}.$$

  - K_{DP} is specific differential phase [deg km^{-1}]
  - Z is reflectivity [mm^6/m^3]
  - S is snow rate [mm h^{-1}]
  - p_0 is a reference pressure of 1013.25 hPa
  - p calculated with radar height assuming a standard atmosphere
    - Results in the coefficient varying from 1.48 in Oklahoma, to 1.61 in Colorado
  - F_o and F_s are calculated with the same canting angle distribution and aspect ratio as the 2018 equation

Experiments with K_{DP} Processing and S(Z) Filling

- K_{DP} is calculated over a 9 (25) gate segment when $Z \geq (<)$ 40 dBZ.
- Three smoothing experiments:
  - None
  - 3 gates by 3 radials
  - 20 gates by 20 radials

- In areas of $K_{DP} < 0.03°/km$, snow rate was calculated as one of the following:
  - $S(K_{DP}, Z)$ (or 0 if $K_{DP} < 0$);
  - $Z=75S^2$;
  - Dynamically fitted Z-$S(K_{DP}, Z)$ using data in areas of $K_{DP} \geq 0.03°/km$.

Unsmoothed Kdp

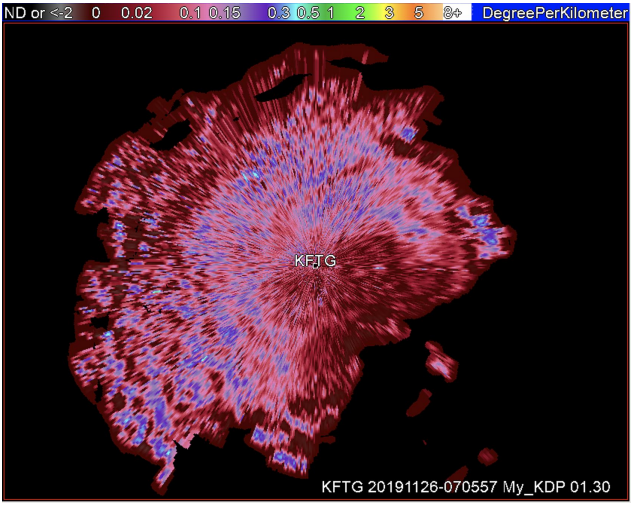

3x3 smoothed Kdp

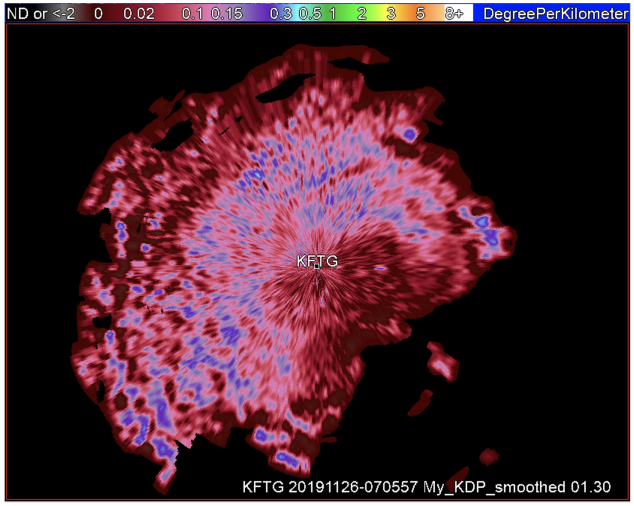

20x20 smoothed Kdp

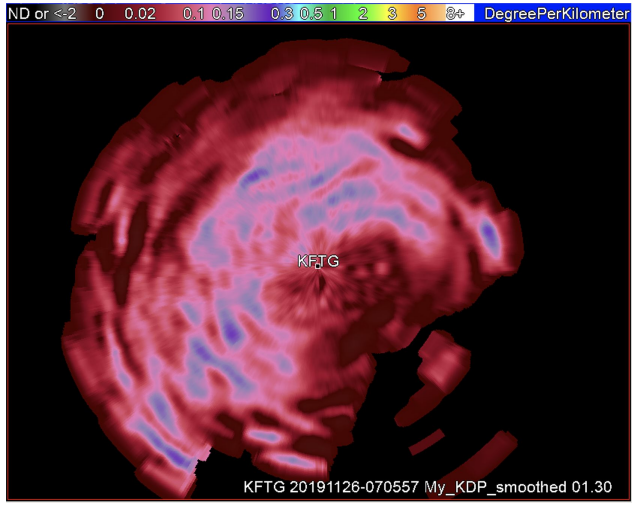

“Hybrid Scan” of S(K_{DP}, Z)

- Prior analysis (not shown here) found that S(K_{DP}, Z) was more accurate at higher tilts closer to the radar, and at the 0.5° tilt at further ranges from the radar
- The “Hybrid Scan” blends the 1.3° tilt (or closest tilt) with the 0.5° tilt
  - Using only 1.x° QPE for $r < 30$ km
  - Using only 0.5° QPE for $r \geq 50$ km
  - Linearly blending 0.5° and 1.x° for $30 \leq r < 50$ km

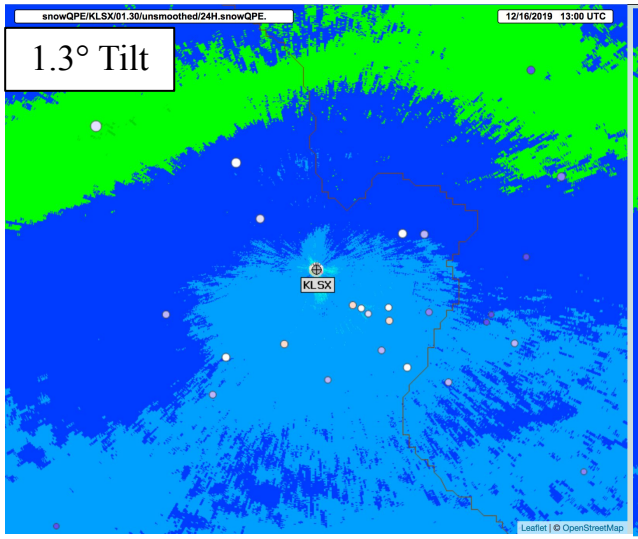

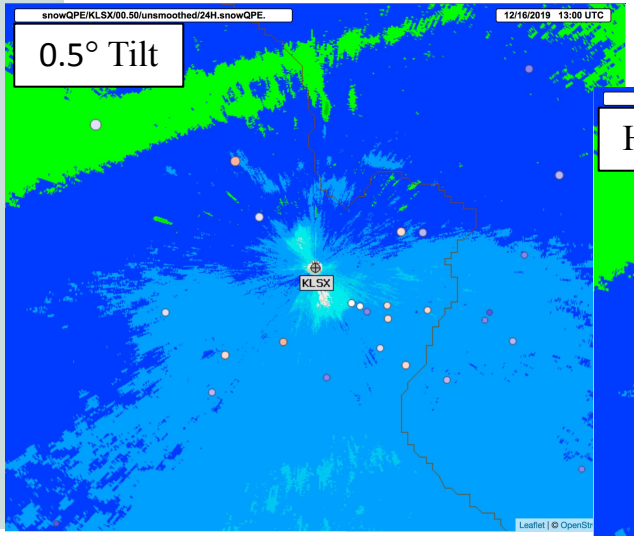

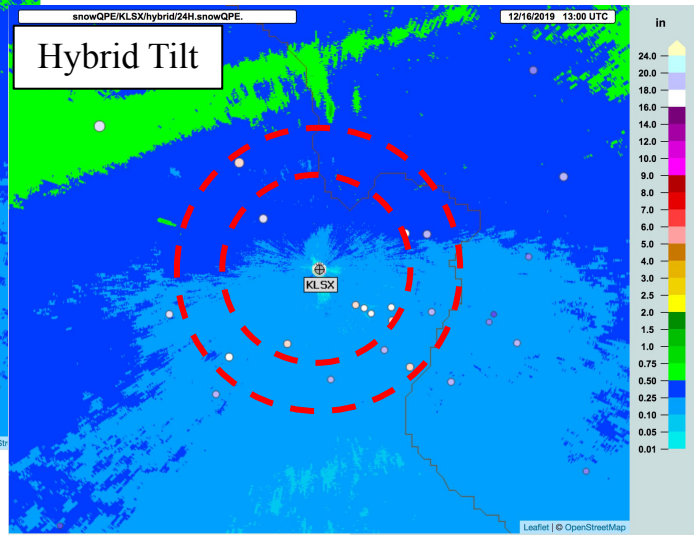

Case Example: 16 December 2019

- Snowstorm produced over 6” across Kansas
- Surface temperatures were around -5°C in a nearly saturated environment

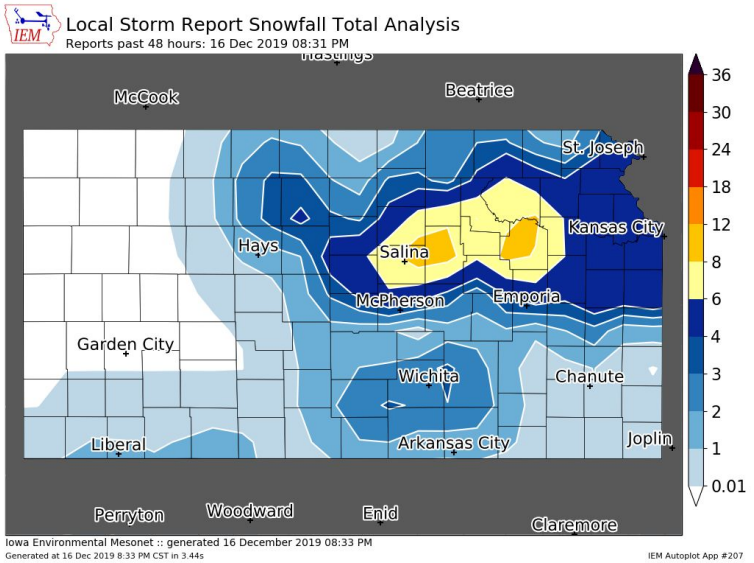

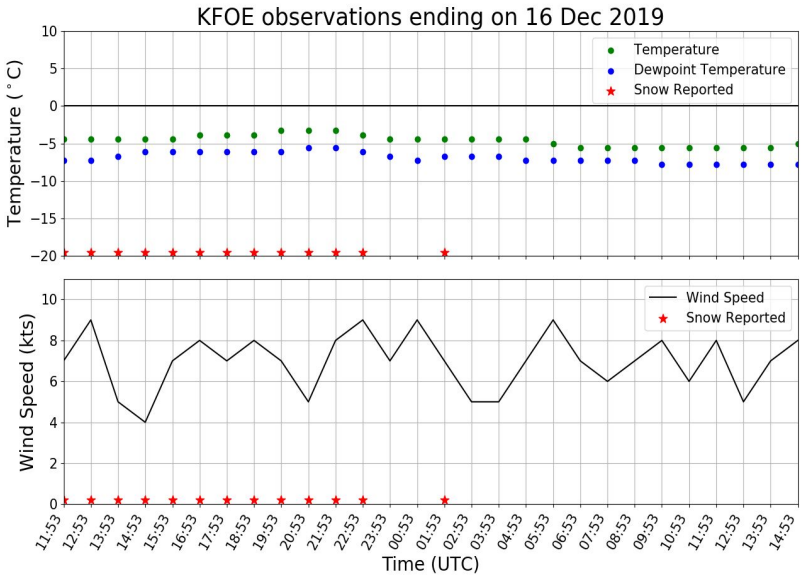

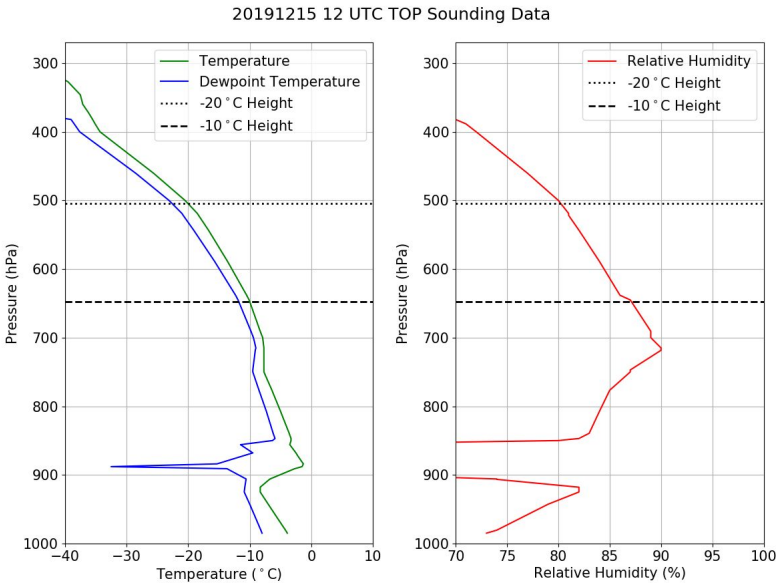

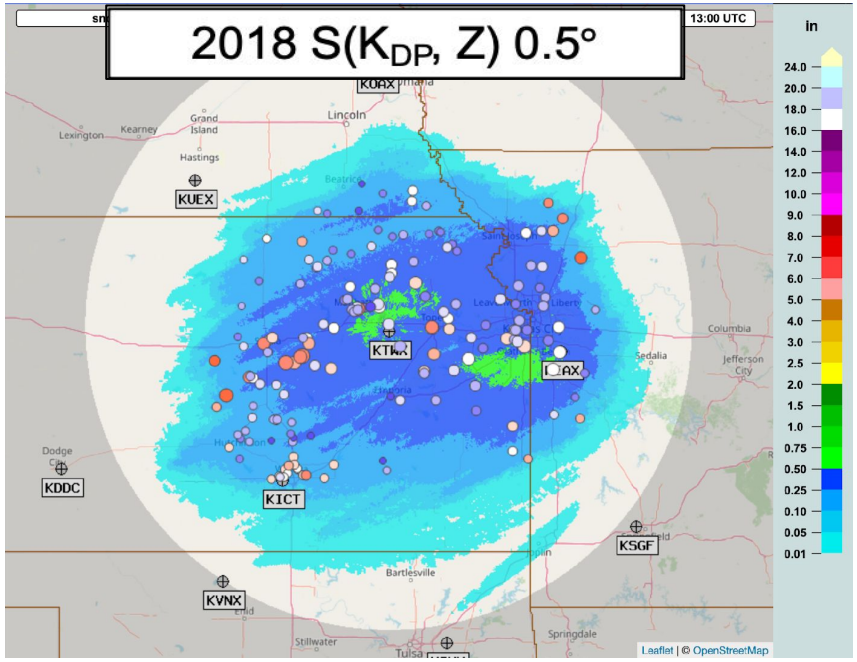

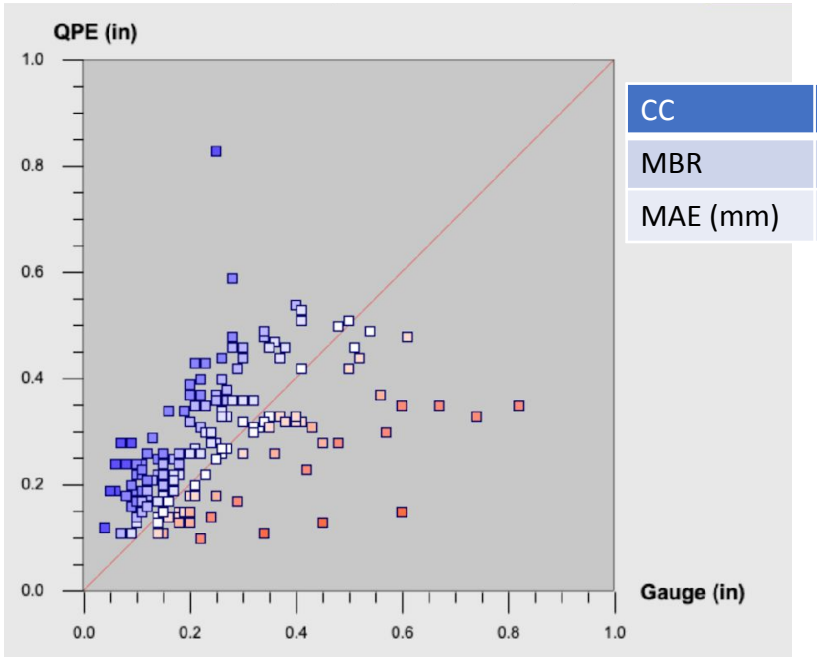

CC	0.531
MBR	1.138
MAE (mm)	2.540

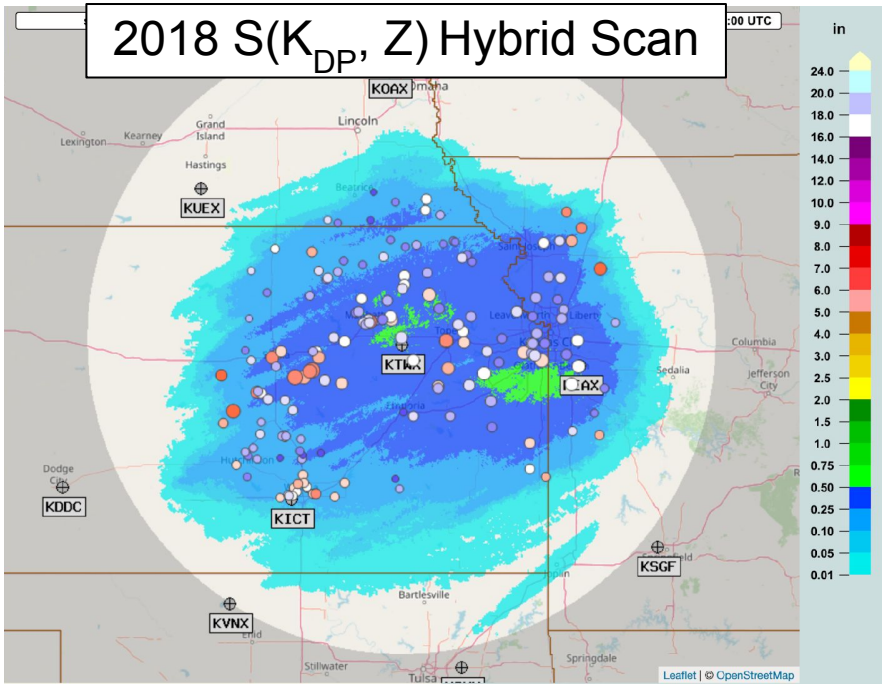

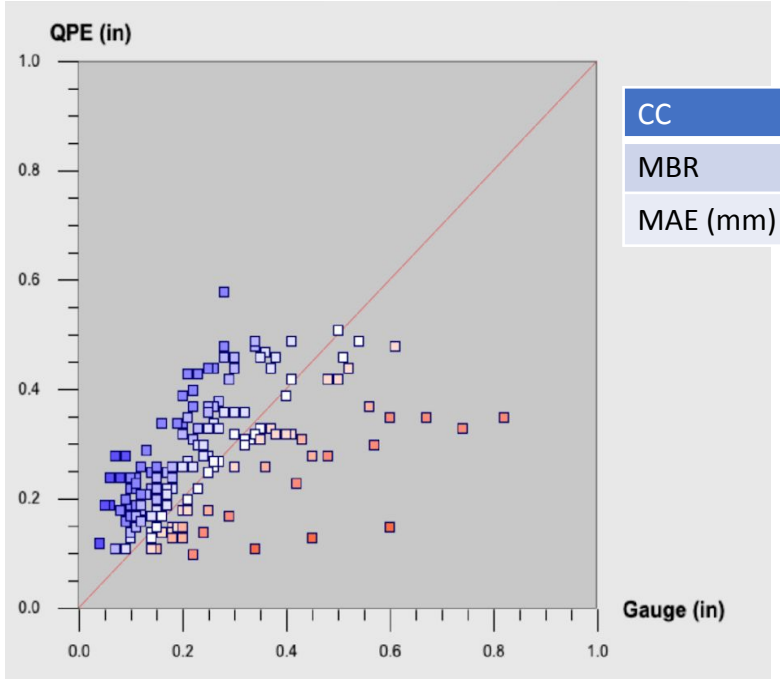

CC	**0.563**
MBR	**1.117**
MAE (mm)	**2.413**

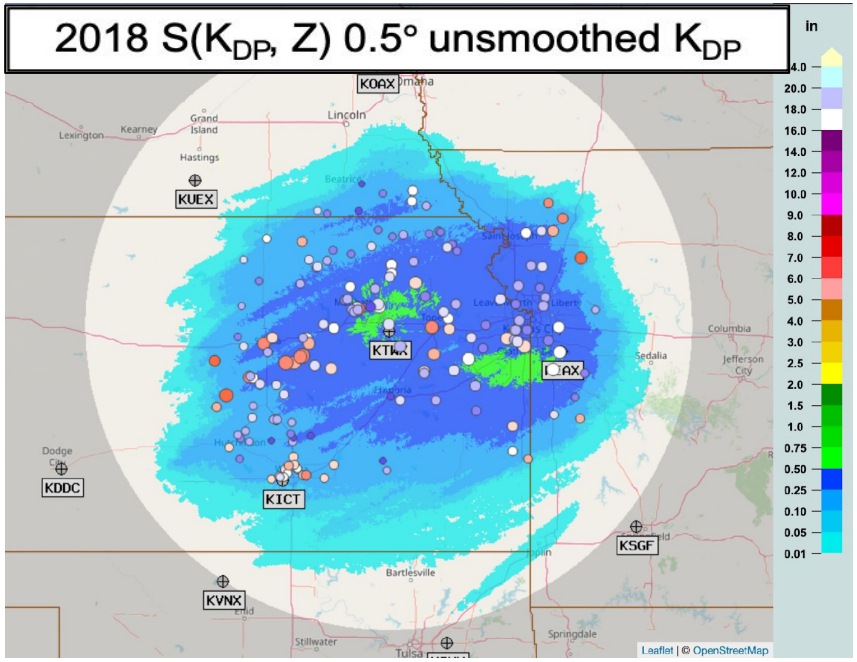

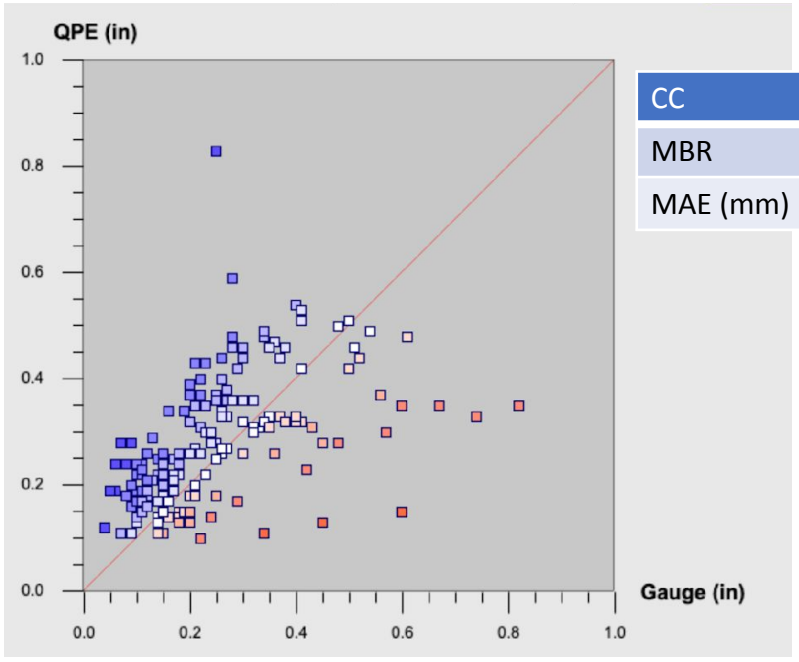

CC	0.531
MBR	1.138
MAE (mm)	2.540

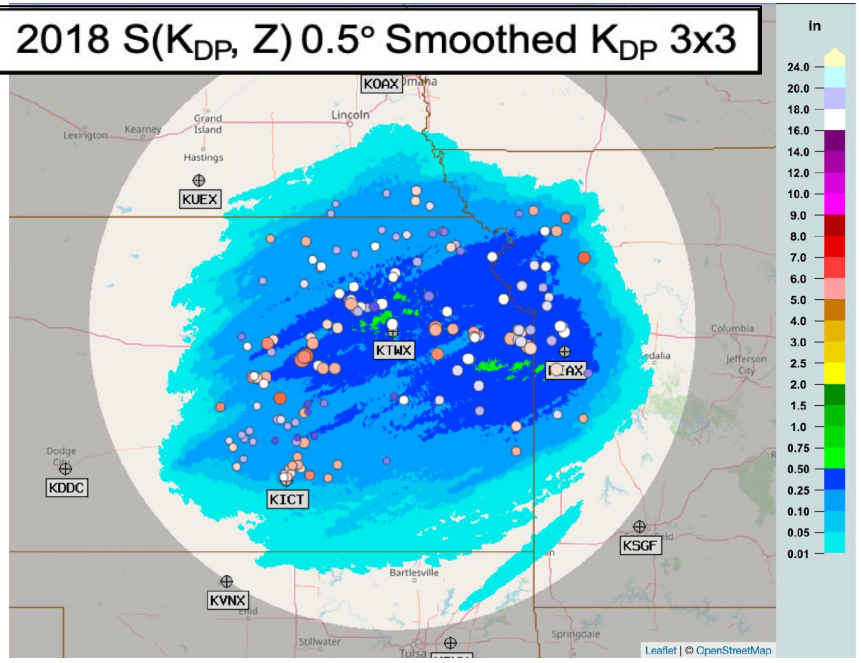

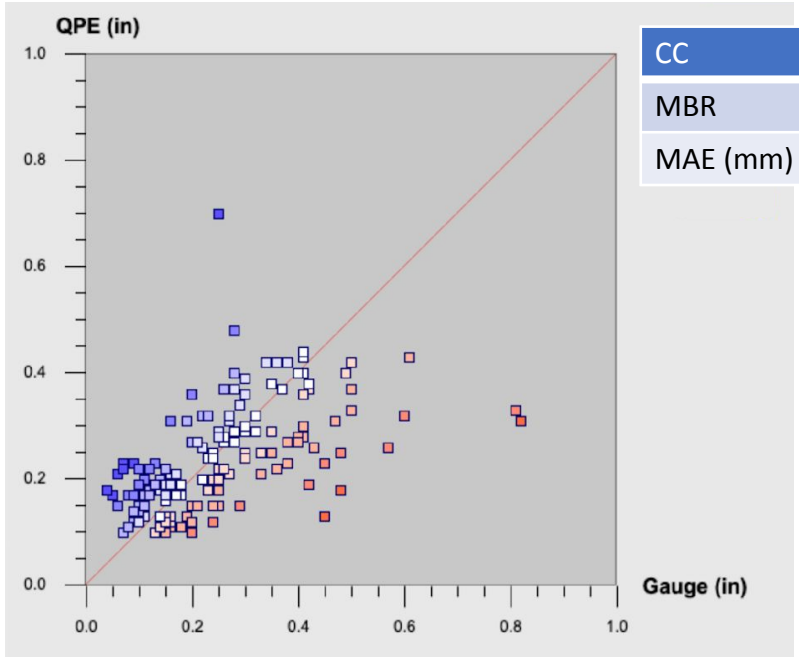

CC	**0.578**
MBR	**0.954**
MAE (mm)	**2.108**

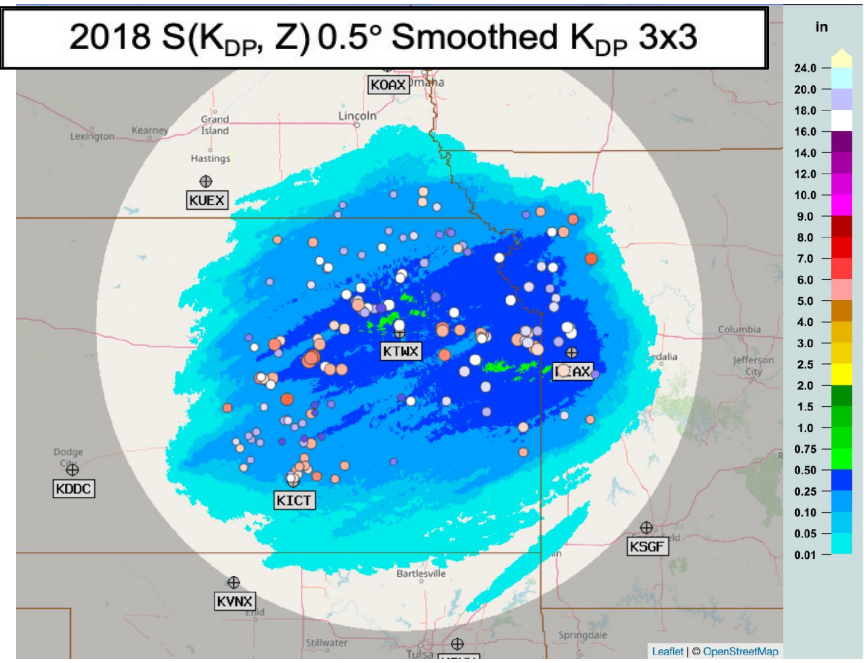

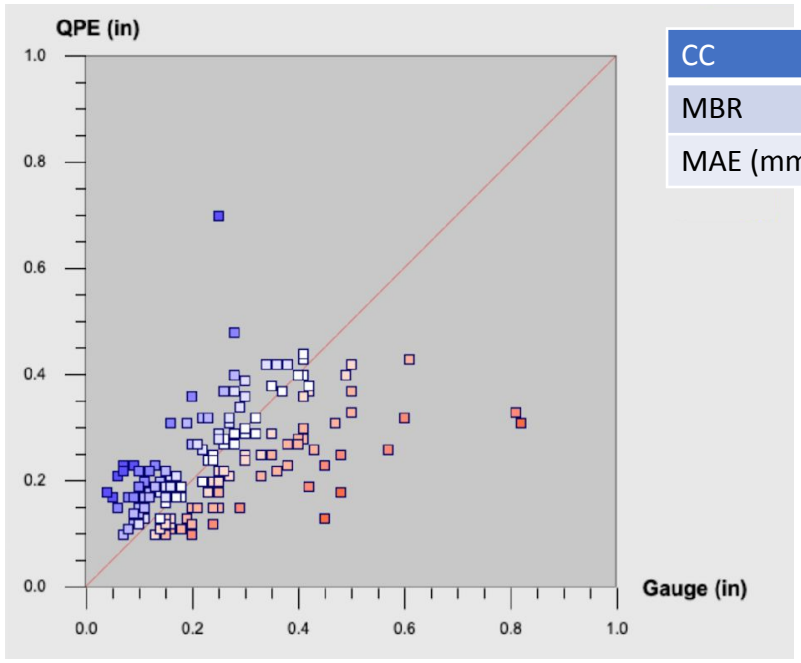

CC	0.578
MBR	**0.954**
MAE (mm)	2.108

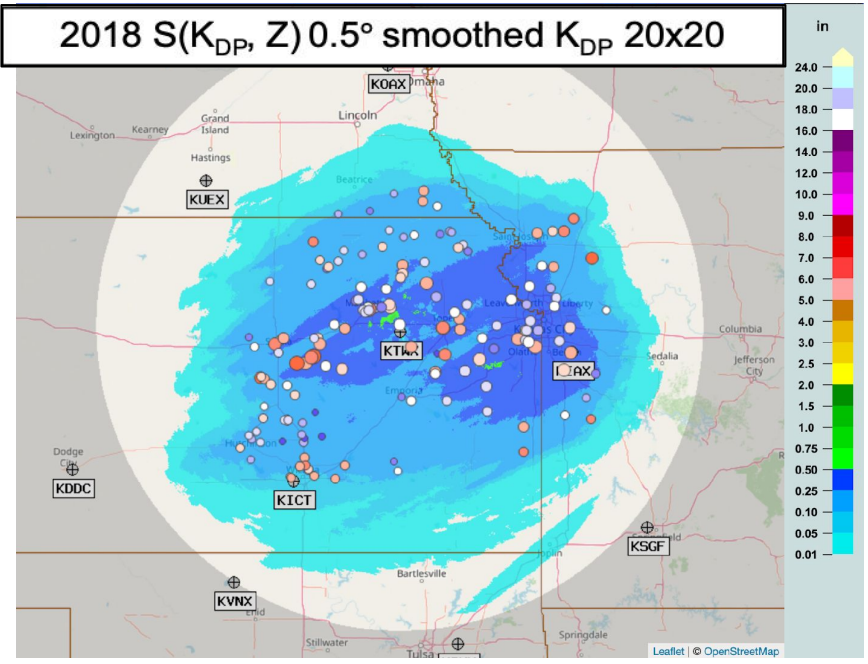

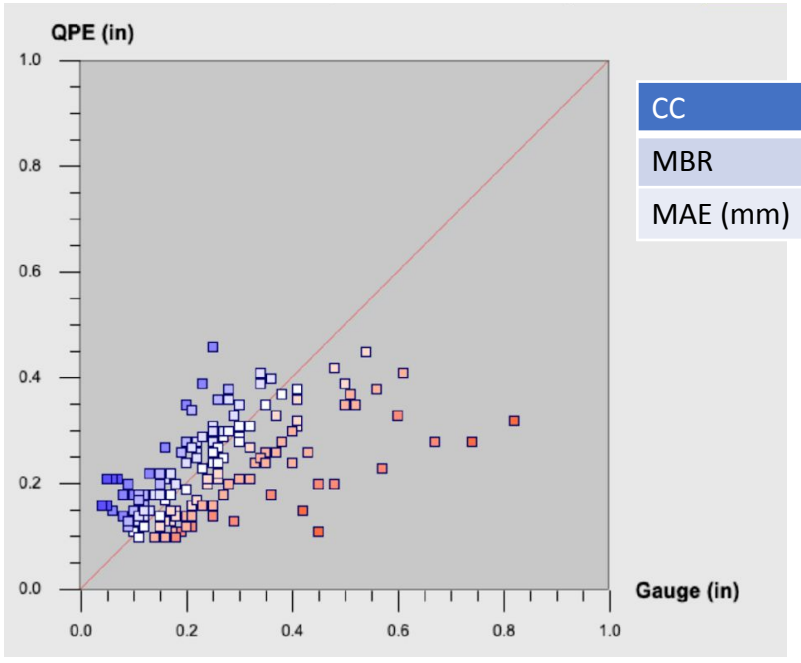

CC	**0.618**
MBR	0.905
MAE (mm)	**2.057**

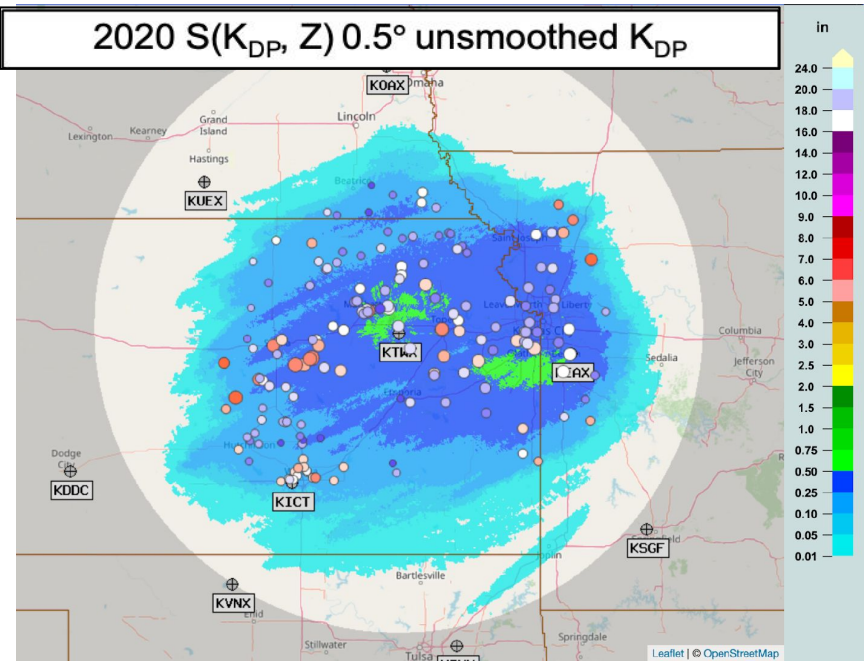

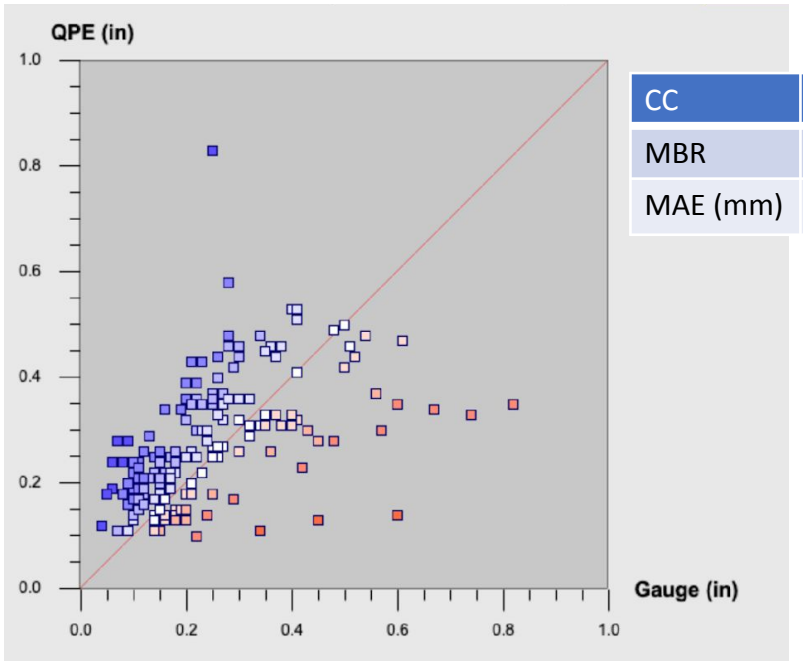

2018

CC	0.528	*0.531*
MBR	**1.129**	*1.138*
MAE (mm)	**2.515**	*2.540*

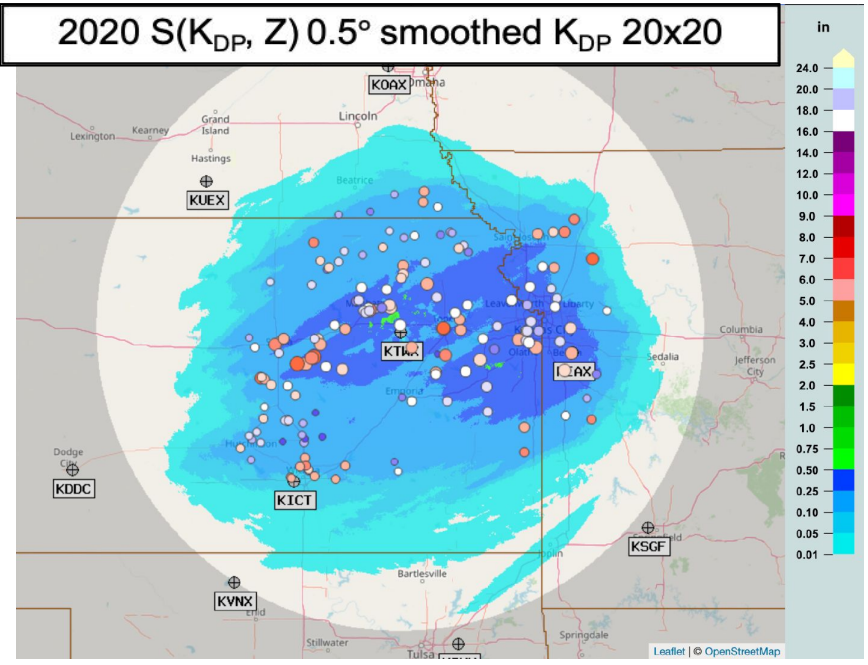

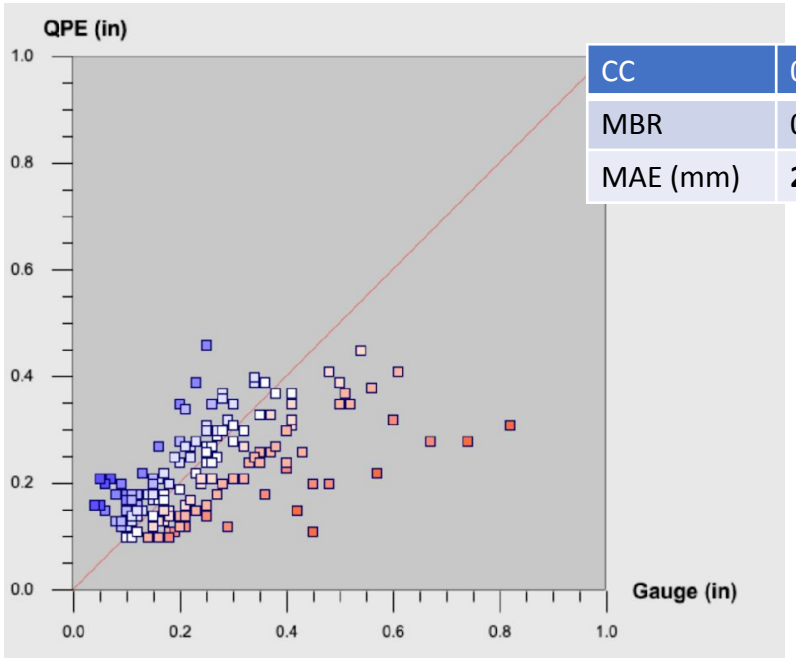

2018

CC	0.617	*0.618*
MBR	0.897	***0.905***
MAE (mm)	**2.057**	***2.057***

2020 S(K_{DP}, Z) 0.5° unsmoothed K_{DP}

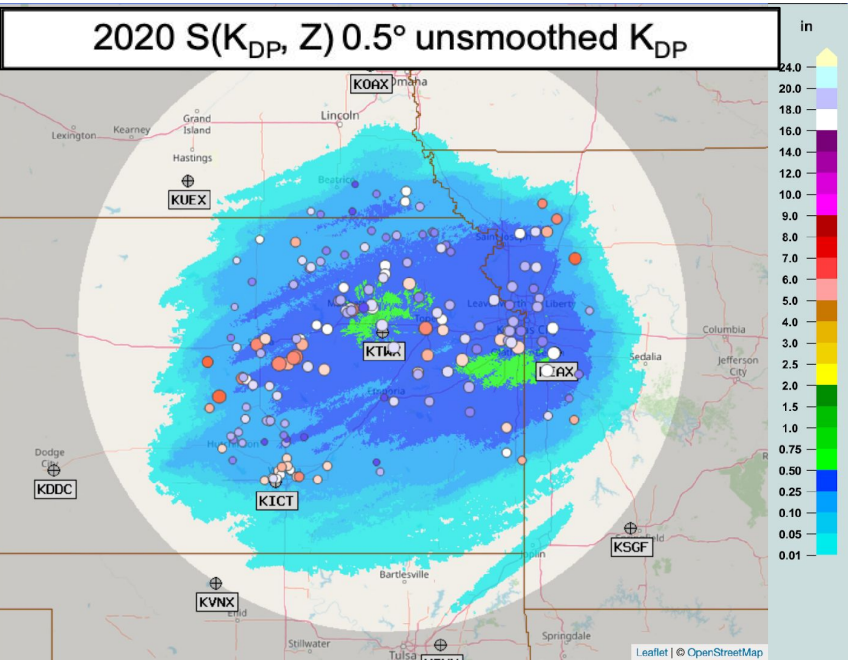

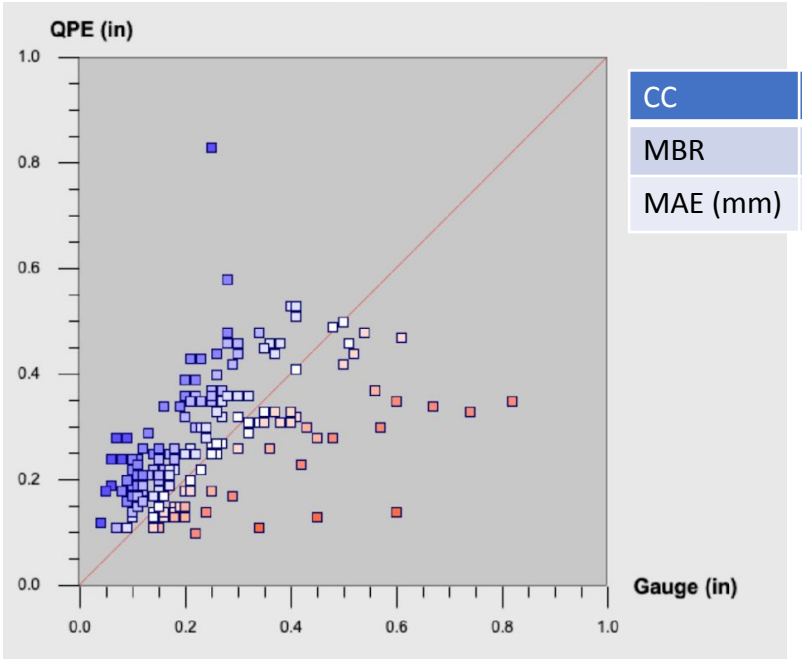

CC	0.528
MBR	1.129
MAE (mm)	2.515

2020 S(K_{DP}, Z) hybrid unsmoothed K_{DP} Dy S(Z)

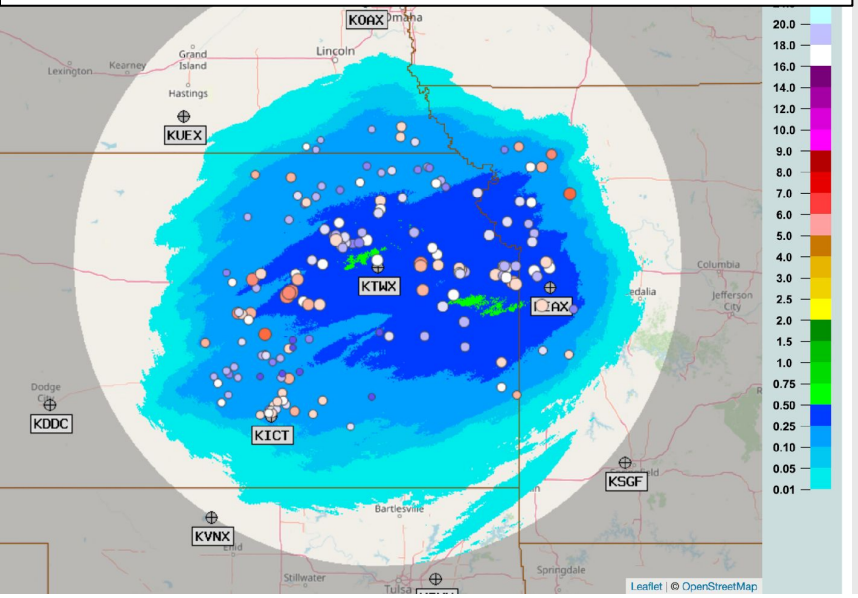

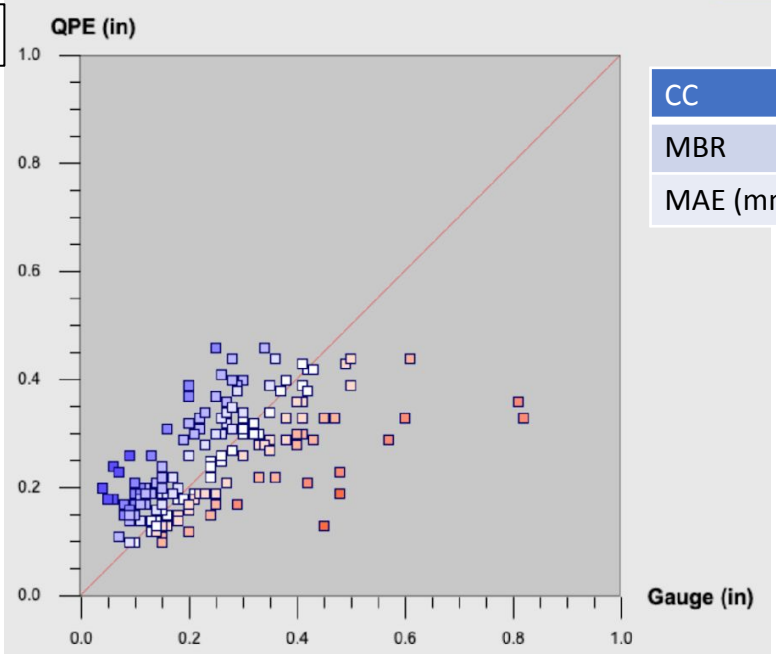

CC	**0.645**
MBR	**1.020**
MAE (mm)	**1.981**

PPS

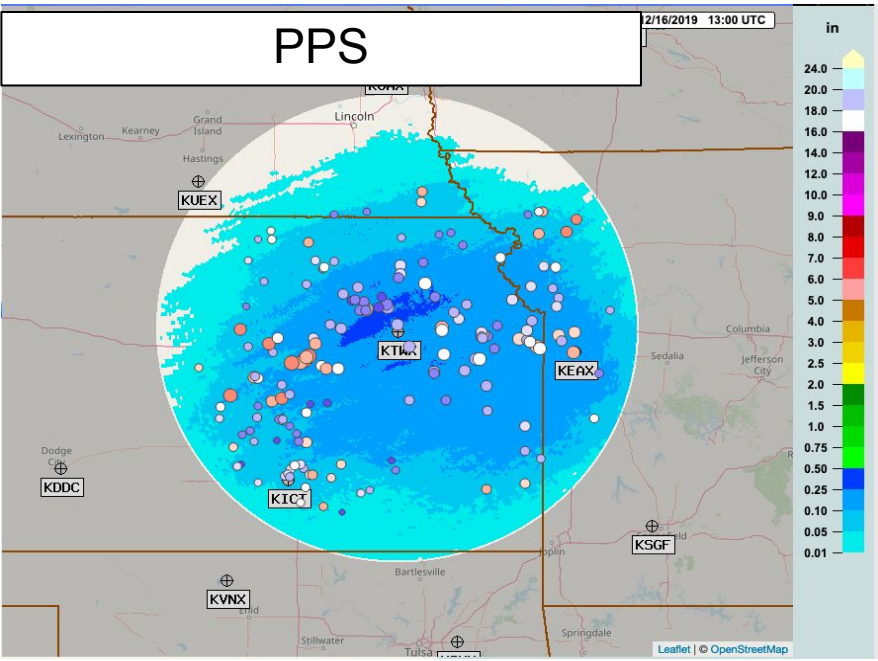

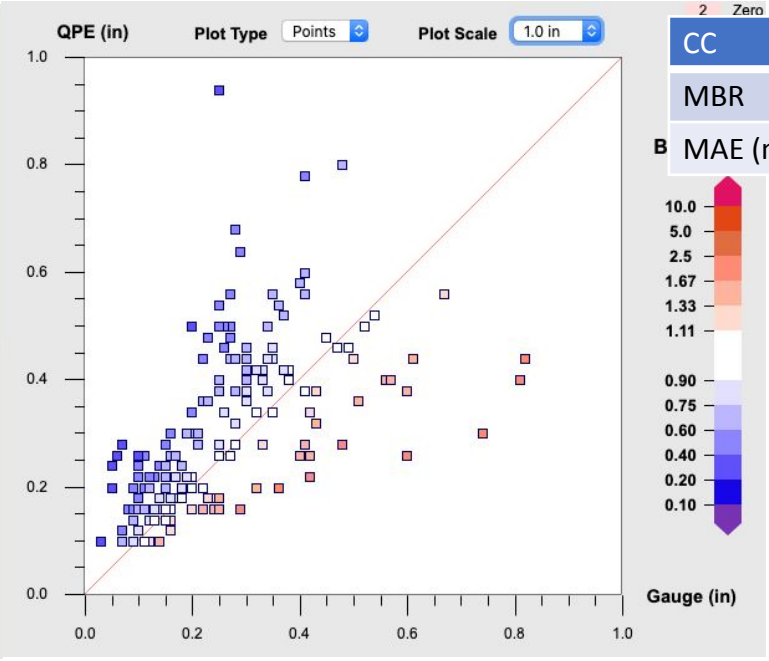

CC	0.552
MBR	1.197
MAE (mm)	2.896

2020 S(K_{DP}, Z) hybrid unsmoothed K_{DP} Dy S(Z)

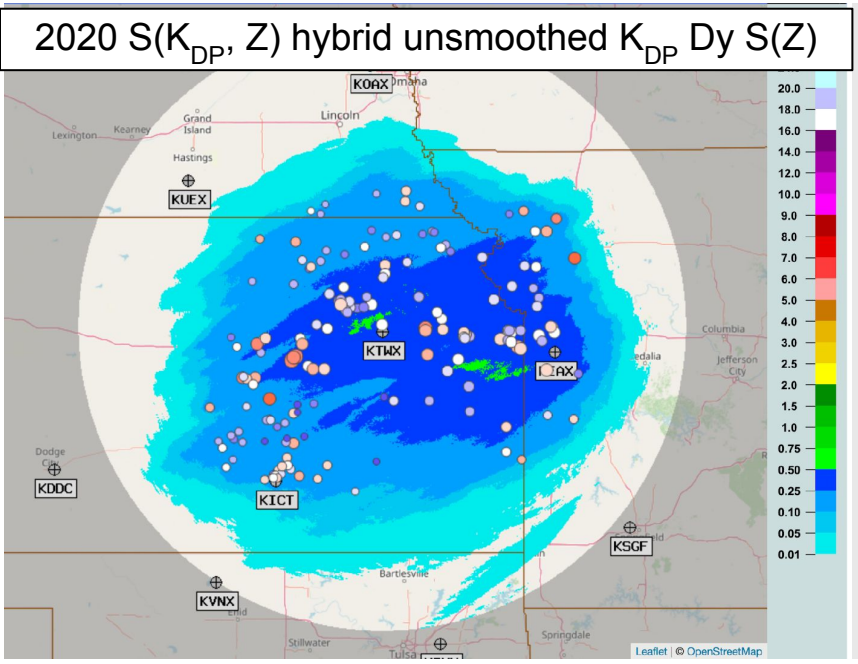

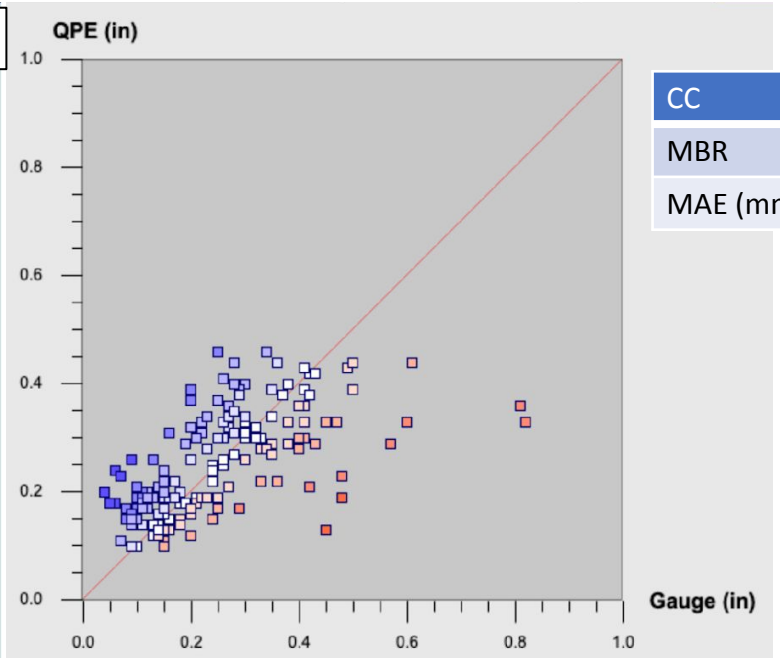

CC	**0.645**
MBR	**1.020**
MAE (mm)	**1.981**

All Event Average Stats

$S(K_{DP}, Z)$ Eqn.	Hybrid Scan	K_{DP}-Smoothing		Bias (Q/G)	MAE (mm)
PPS	**Hybrid**			**0.966**	**5.050**
2018		N	N	1.007	5.134
2018		N	N	1.017	5.055*
2018		3x3	N	0.868	5.440
2018		20x20	N	0.843	5.022
2018		20x20	Dynamic S-Z	0.823	5.260
2018		N	Dynamic S-Z	0.981	5.354
2020		N	N	0.932	5.166
2020		N	$75S^2$	1.097	5.317
2020		N	Dynamic S-Z	1.156	5.522
2020		20x20	N	0.845	5.011
2020		20x20	$75S^2$	0.928	4.933*
2020		20x20	Dynamic S-Z	0.963	4.953*
2020		20x20	Dynamic S-Z	0.945	5.102*
2020		3x3	Dynamic S-Z	1.052	5.535
2020		3x3	Dynamic S-Z	1.061	5.453

- $S(K_{DP}, Z)$ with 20x20 K_{DP} - smoothing consistently improves the MAE over the S(Z) QPE
- K_{DP} - smoothing introduced underestimation, especially for the 2018 Eqn.
- S(Z) filling combined with 20x20 K_{DP} - smoothing help reduce random errors, but introduced dry bias for 2018 Eqn.
- Next steps:
  - Detailed investigations of large local errors in selected events
  - Expanding case studies with the best performing schemes

Mean absolute error for all events

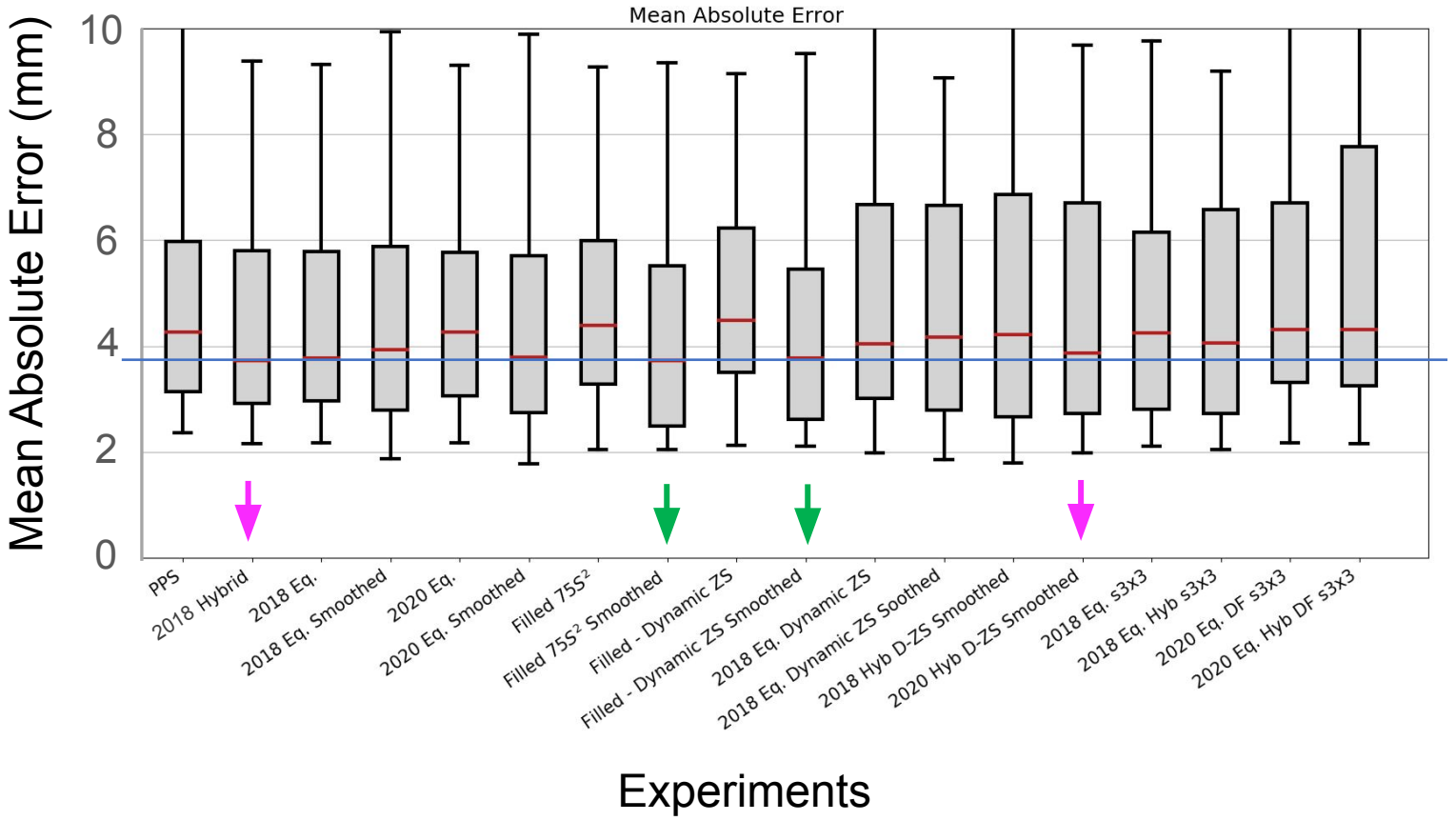

Mean bias ratio for all events

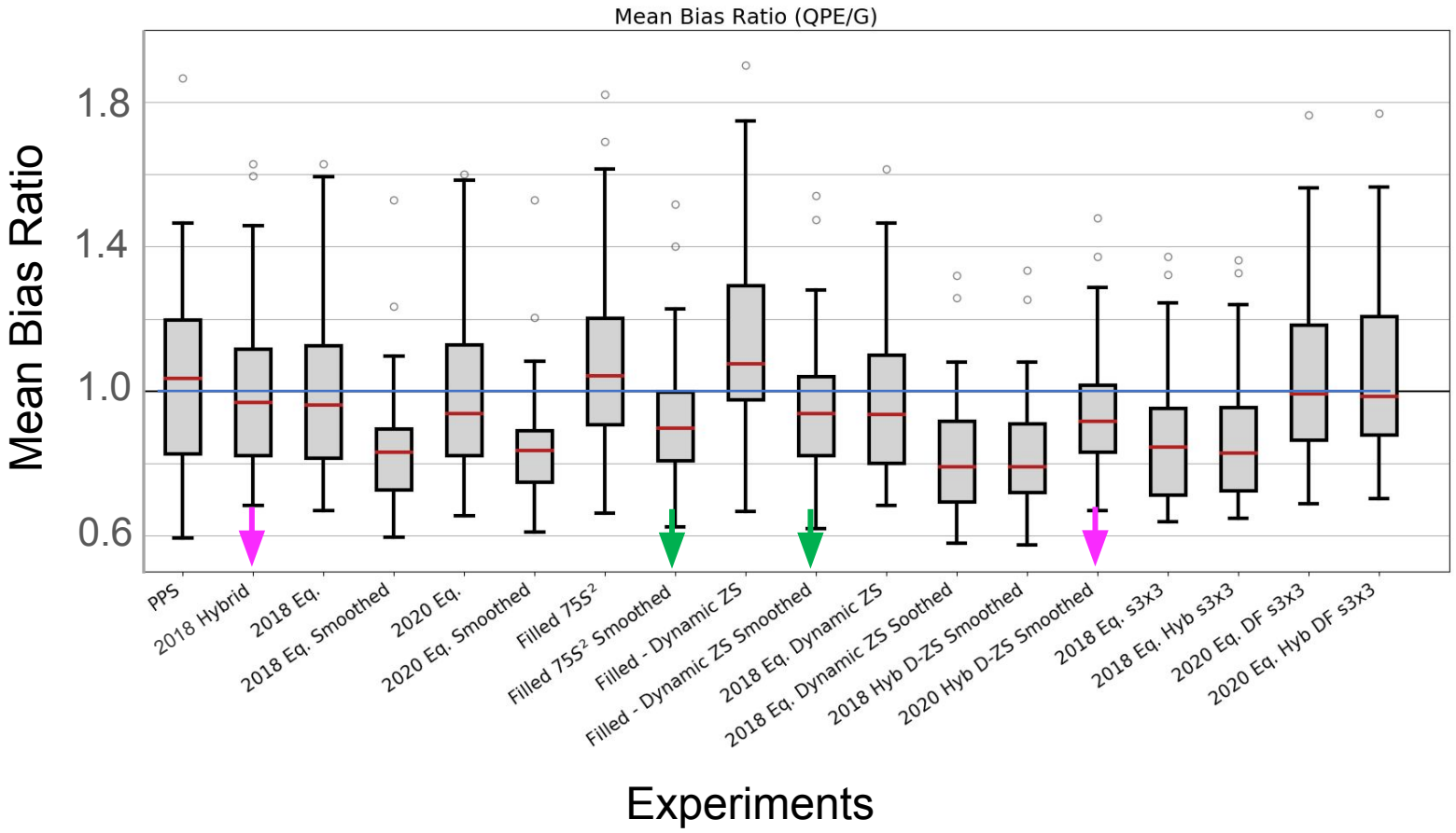

Conclusions

- Variability of the S(Z) relations is prohibitively large
- S(Kdp, Z) derived from OK 2DVD snow measurements using wide range of b/a from 0.5 to 0.8, and σ form 0 to 40 deg
- S(Kdp, Z) relation's multiplier dependent on particle shape, and orientation – change in density is partially accounted for
- S(Kdp, Z) relation's exponents are almost invariant to particle shape and orientation

Conclusions

- Aggressive spatial averaging is required to obtain robust estimates of polarimetric variables in snow at S band – polarimetric algorithms depends on reliable Kdp and Z

- Polarimetric relations for snowfall estimation are tested for several moderate/heavy snow events – show good potential for improvement in radar snow QPE

- Further optimization and testing of polarimetric algorithms for snow QPE is needed to mitigate the existing deficiencies

Auxiliary slides

σ – KOUN RHI, 2007-06-26, 1202 UTC

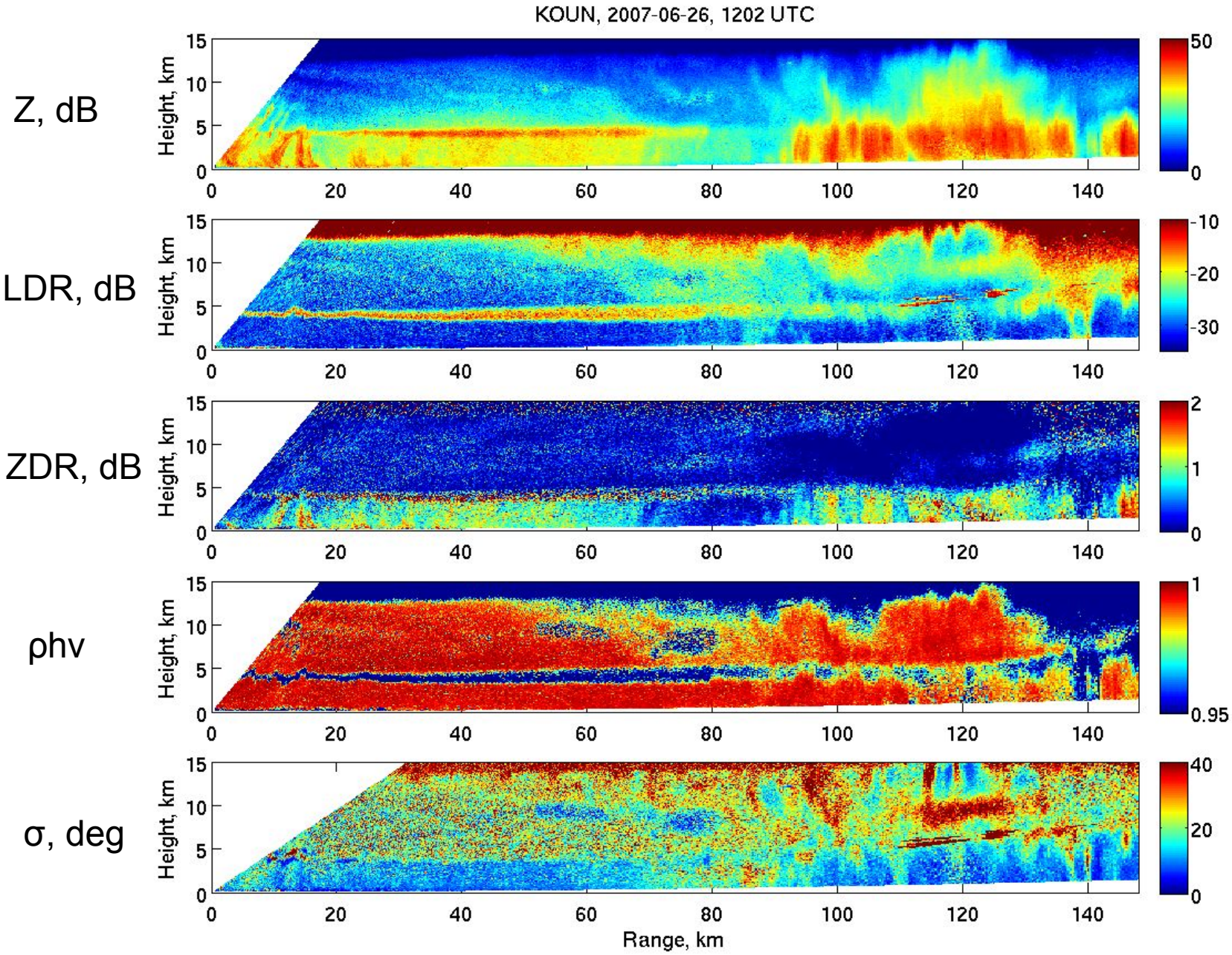

σ – KOUN RHI, 2007-06-26, 1257 UTC

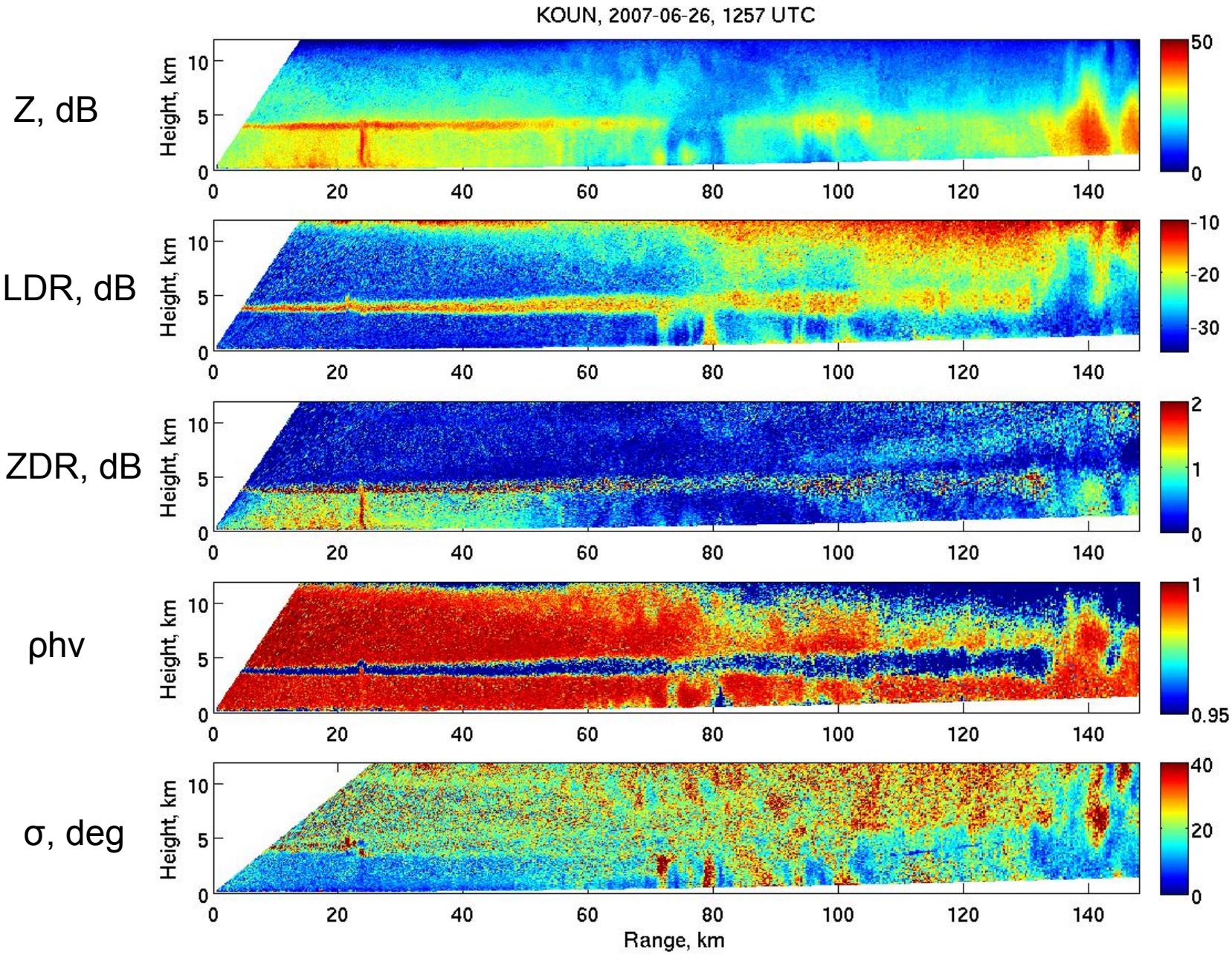

σ – PECAN SPOL RHI, 2015-06-12

Z, dB

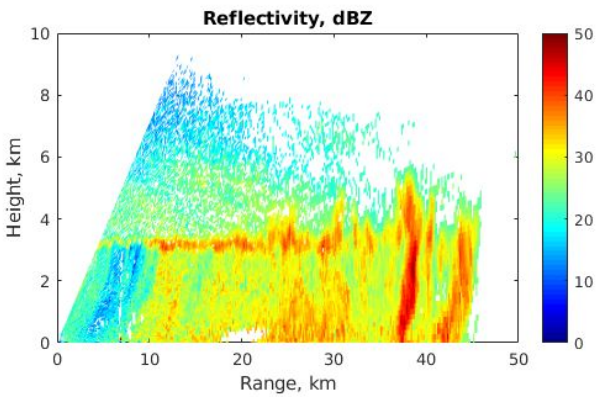

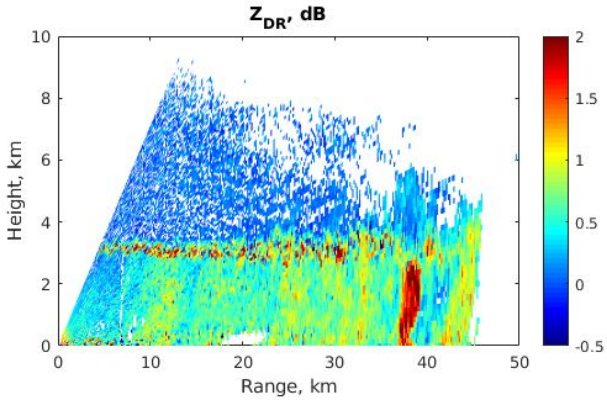

ZDR, dB

ρhv

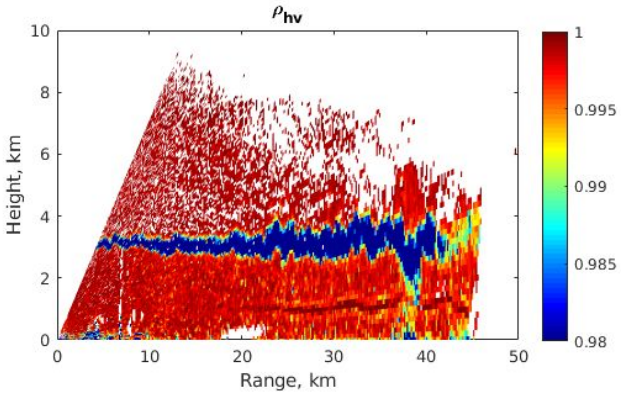

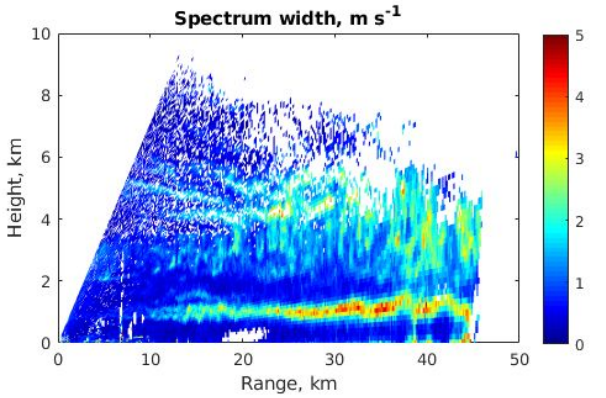

SW, m s^{-1}

LDR, dB

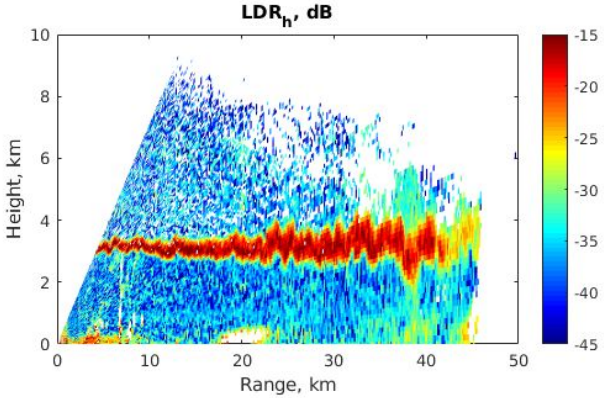

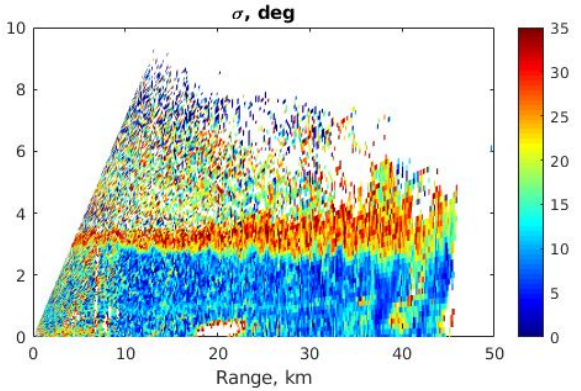

σ, deg

Snowfall rates and accumulations from 2.4° PPI, KGJX, 2013-01-28

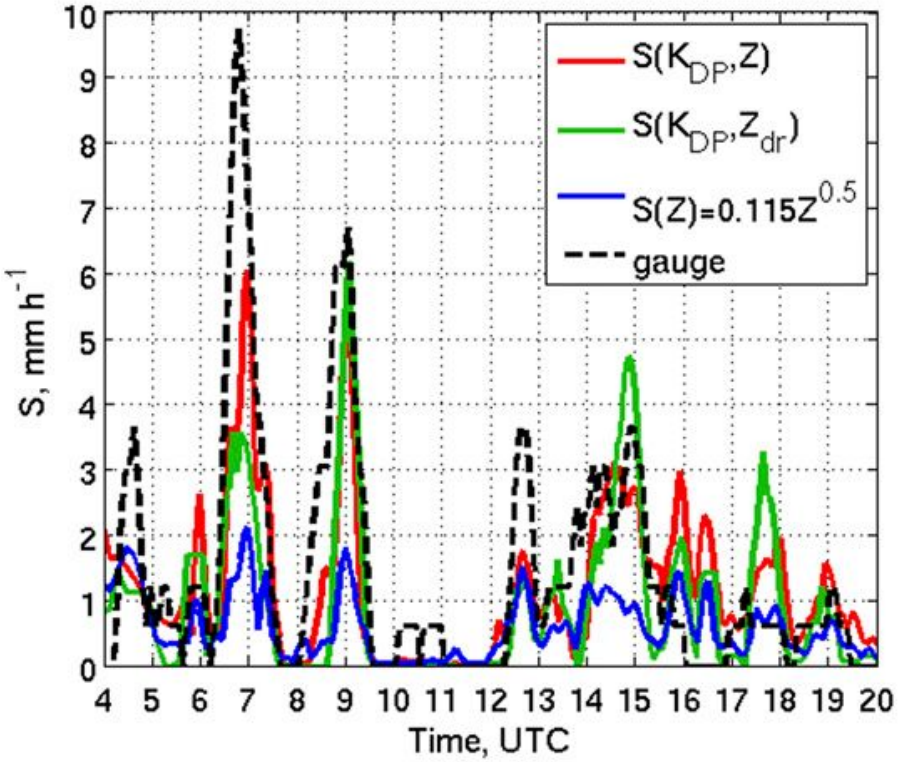

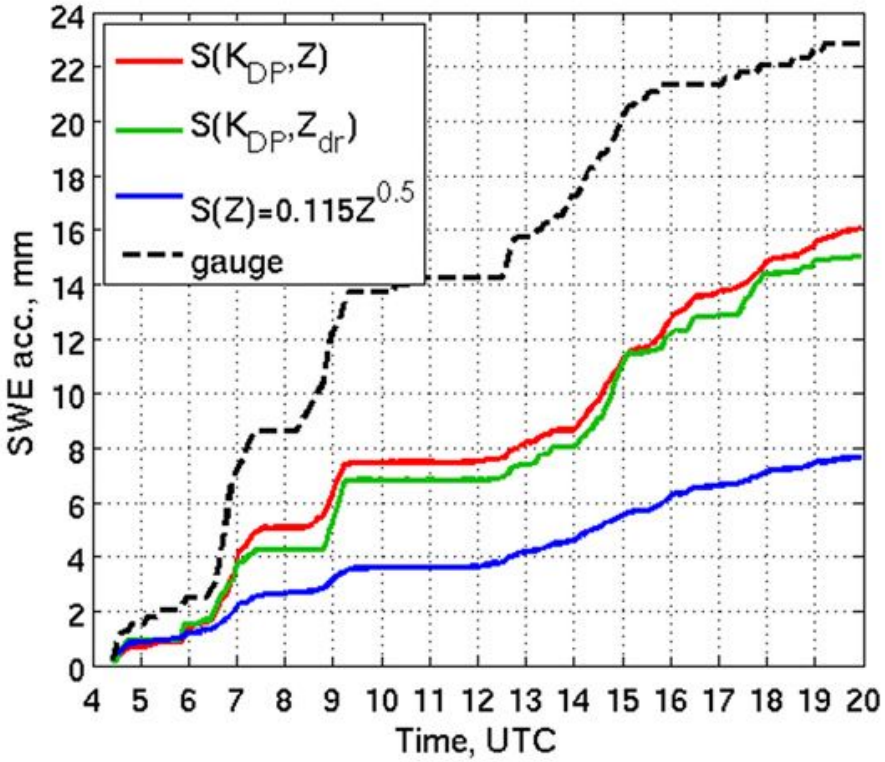

- S(Kdp, Z) – moderately close to the gauge measurement; most realistic peaks in S
- S(Kdp, Zdp) – moderately close to the gauge measurement, slightly worse than S(Kdp, Z)
- S(Z) – heavily underestimates S, maximum < 2.1 mm/h

Snowfall rates and accumulations adjusted for b/a and σ, 2.4° PPI, KGJX,

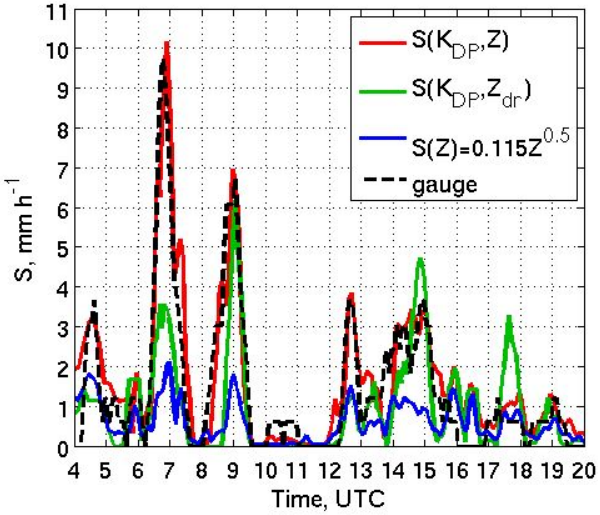

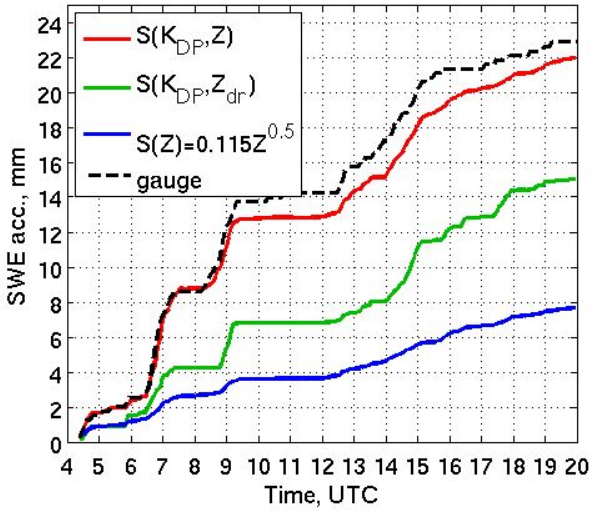

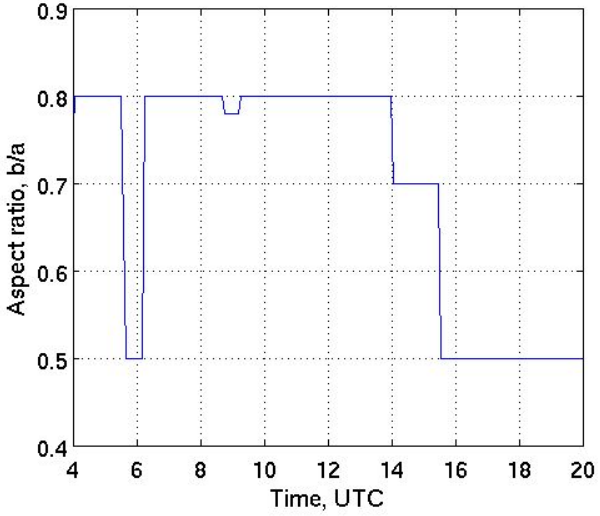

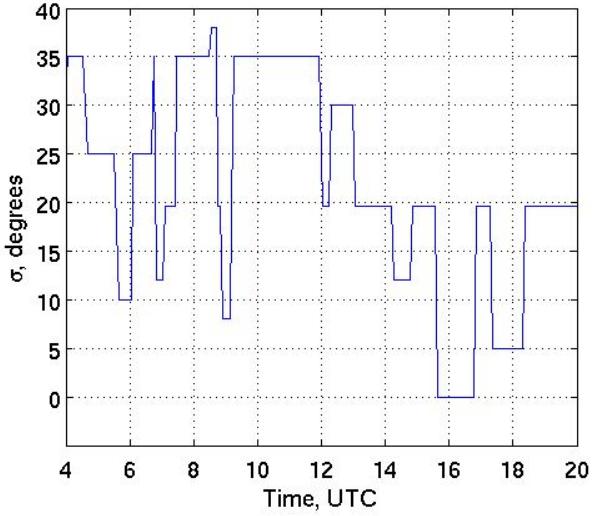

S(KDP, Z) tunable – much better comparison with gauge for “optimal” b/a and σ

Thank you!

Questions?

petar.bukovcic@noaa.gov

References

Ryzhkov, A., P. Zhang, H. Reeves, M. Kumjian, T. Tschallener, S. Troemel, and C. Simmer, 2016: Quasi-Vertical Profiles - A New Way to Look at Polarimetric Radar Data. *J. Atmos. Oceanic Technol.*, **33**, 551-562, doi:10.1175/JTECH-D-15-0020.1

Tobin, D.M. and M.R. Kumjian, 2017: Polarimetric Radar and Surface-Based Precipitation-Type Observations of Ice Pellet to Freezing Rain Transitions. *Wea. Forecasting,* **32**, 2065–2082, https://doi.org/10.1175/WAF-D-17-0054.1

Ryzhkov, A., Bukovčić, P., Murphy, A., Zhang, P., and McFarquhar, G., 2018: Ice microphysical retrievals using polarimetric radar data. In 10th European Conference on Radar in Meteorology and Hydrology, 1–6 July, Netherlands, # 40, 2018. https://projects.knmi.nl/erad2018/ERAD2018_extended_abstract_040.pdf

Murphy, A., A. Ryzhkov, and P. Zhang, 2020: Columnar Vertical Profiles (CVP) methodology for validating polarimetric radar retrievals in ice using in situ aircraft measurements. *J. Atmos. Oceanic Tech*., 37, 1623-1642, https://doi.org/10.1175/JTECH-D-20-0011.1.

Bukovčić, P., A. Ryzhkov, and D. Zrnić, 2020: Polarimetric relations for snow estimation – radar verification. *J. Appl. Meteor. Climatol.,* 202**0**, https://doi.org/10.1175/JAMC-D-19-0140.1